Charles University in Prague

Faculty of Science

Study program: Physical chemistry

Mgr. Pavla Eliášová

SYNTHESIS, CHARACTERIZATION AND CATALYTIC APPLICATION OF NOVEL ZEOLITES

Dissertation

Supervisor: Prof. Ing. Jiří Čejka, DrSc.

Prague, 2014

Univerzita Karlova v Praze

Přírodovědecká fakulta

Studijní program: Fyzikální chemie

Mgr. Pavla Eliášová

SYNTÉZA, CHARAKTERIZACE A KATALYTICKÉ VYUŽITÍ NOVÝCH TYPŮ ZEOLITŮ

Disertační práce

Školitel: Prof. Ing. Jiří Čejka, DrSc.

Praha, 2014

Prohlášení:

Na dizertační práci jsem pracovala na oddělení Syntézy a katalýzy na Ústavu fyzikální chemie J. Heyrovského AV ČR.

Prohlašuji, že jsem závěrečnou práci zpracovala samostatně a že jsem uvedla všechny použité informační zdroje a literaturu. Tato práce ani její podstatná část nebyla předložena k získání jiného nebo stejného akademického titulu.

V Praze, 20.2.2014

Podpis

ACKNOWLEDGEMENT

I would like to thank to my supervisor, Prof. Jiří Čejka, for offering me an opportunity to work on my thesis at the Academy of Science and I am deeply grateful for his advices and support during my studies. I highly regard working under his guidance.

My thanks also belong to Dr. Wieslaw J. Roth for his help, advices and inspiration regarding the whole zeolite science. I would like to thank Ing. Lenka Kurfiřtová and Ing. Naděžda Žilková for catalytic measurements and GC analyses, PhD. Martin Kubů and Ing. Arnošt Zukal, CSc. for nitrogen and argon adsorption measurement and for useful advices and help with the results discussion, PhD. Dana Vitvarová for measuring FTIR, Dr. Oleksiy V. Shvets and PhD. Mariya V. Shamzy for synthesis and advices about the synthesis of UTL zeolite, Assoc. Prof. Petr Nachtigall for theoretical calculations, RNDr. Libor Brabec, CSc. for taking SEM images, Prof. Russell Morris for my supervising in St. Andrews, and Prof. Wuzong Zhou and BSc. Heather F. Greer for taking HRTEM images.

Also, I would like to thank all people and colleagues, who helped and supported me during my work.

List of abbreviations

BEA	three-dimensional zeolite with 12-12-12-ring channel system
BET	the method used for the calculation of surface areas of solids (m^2/g) by physical adsorption of gas molecules; based on the Brunauer, Emmett, and Teller theory
BJH	pore size model developed by Barret, Joyner, and Halenda; based on the modified Kelvin equation corrected for multilayer adsorption
CD_3CN	deuterated acetonitrile
$C_{16}TMA$	hexadecyltrimethylammonium cation
D3R	double-three-ring, secondary building unit of zeolites
D4R	double-four-ring, secondary building unit of zeolites
DEDMS	diethoxydimethylsilane
EDX	Energy dispersive X-ray spectroscopy
FTIR	Fourier transform infrared spectroscopy
FWHM	full width at half-maximum
HRTEM	high resolution transmission electron microscopy
i-PrOH	isopropyl alcohol
IEZ	interlamellar expanded zeolite
IPC	Institute of Physical Chemistry
IPC-1P	two-dimensional lamellar material prepared by hydrolysis from UTL
IPC-1PI	two-dimensional pillared material prepared from IPC-1P
IPC-2	three-dimensional zeolite with 12-10-ring channel system
IPC-4	three-dimensional zeolite with 10-8-ring channel system
IPC-6	three-dimensional zeolite with 12-10-ring and 10-8-ring channel system
MAS NMR	magic angle spinning nuclear magnetic resonance
MFI	three-dimensional zeolite with 10-10-10-ring channel system
PCR	Prague Chemistry fouR
pK_a	logarithmic acid dissociation constant
SDA	structure directing agent
SEM	scanning electron microscopy
Si/Al	silicon to aluminium molar ratio
Si/Ge	silicon to germanium molar ratio
TEOS	tetraethyl orthosilicate
T-O-S	time-on-stream (min)
TPA	tetrapropyl ammonium
V_{mic}	micropore volume

V_{tot}	total pore volume
WHSV	weight hour space velocity (h^{-1})
XRD	X-ray powder diffraction
ε (B)	extinction coefficient for Brønsted acid sites (cm/µmol)
ε (L)	extinction coefficient for Lewis acid sites (cm/µmol)
2D	two-dimensional
3D	three-dimensional

List of publications

The PhD thesis is based on the following publications:

1) Roth W.J., Shvets O.V., Shamzhy M., Chlubná P., Kubů M., Nachtigall P., Čejka J.;
Postsynthesis Transformation of Three-Dimensional Framework into a Lamellar Zeolite with Modifiable Architecture;
Journal of American Chemical Society, 2011, 133, 6130-6133

2) Shamzhy M.V., Shvets O.V., Opanasenko M.V., Yaremov P.S., Sarkisyan L.G., Chlubná P., Zukal A., Marthala V.R., Hartmann M., Čejka J.;
Synthesis of isomorphously substituted extra-large pore UTL zeolites;
Journal of Materials Chemistry, 2012, 22, 15793-15803

3) Chlubná P., Roth W.J., Greer H.F., Zhou W., Shvets O., Zukal A., Čejka J., Morris R.E.;
3D to 2D routes to ultrathin and expanded zeolitic materials;
Chemistry of Materials, 2013, 25, 542-547

4) Roth W.J., Nachtigall P., Morris R.E., Wheatley P.S., Seymour V.R., Ashbrook A.E., Chlubná P., Grajciar L., Položij M., Zukal A., Shvets O., Čejka, J.;
A family of zeolites with controlled pore size prepared using a top-down method;
Nature Chemistry, 2013, 5, 628-633

5) Mazur M., Chlubná-Eliášová P., Roth W.J., Čejka J.;
Intercalation chemistry of layered zeolite precursor IPC-1P;
Catalysis Today, 2013, in press, doi: 10.1016/j.cattod.2013.10.051

6) Chlubná-Eliášová P., Tian Y., Pinar A.B., Kubů M., Morris R.E., Čejka J.;
The ADoR mechanism for 3D-2D-3D transformation of germanosilicate IWW zeolite;
Submitted 2014

7) Wheatley P.S., Chlubná-Eliášová P., Greer H.F., Zhou W., Seymour V.R., Ashbrook A.E., Pinar A.B., Čejka J., Morris R.E.;
Staged de-intercalation/reorganisation as a route to zeolites with precisely tuneable porosity;
Submitted 2014

8) Smith R.L., Attfield M.P., Anderson M.W., Eliášová P., Čejka J.;
Atomic Force Microscopy of Novel zeolitic materials prepared by top-down synthesis and ADoR mechanism;
Submitted 2014

Further publications:

9) Chlubná P., Roth W.J., Zukal A., Kubů M., Pavlatová J.;
Pillared MWW zeolites MCM-36 prepared by swelling MCM-22P in concentrated surfactant solutions;
Catalysis Today, 2012, 179, 35-42

10) Roth W.J., Chlubná P., Kubů M., Vitvarová D.;
Swelling of MCM-56 and MCM-22P with a new medium - Surfactant-tetramethylammonium hydroxide mixtures;
Catalysis Today, 2013, 204, 8-14

11) Delgado M.R., Bulánek R., Chlubná P., Arean C.O.;
Brønsted acidity of H-MCM-22 as probed by variable-temperature infrared spectroscopy of adsorbed CO and N_2;
Catalysis Today 2013, in press, doi: 10.1016/j.cattod.2013.013

12) Bulánek R., Kolářová M., Chlubná P., Čejka J.;
Coordination of extraframework Li+ cation in the MCM-22 and MCM-36 zeolite: FTIR study of CO adsorbed;
Adsorption, 2013, 19, 455-463

13) Arean C.O., Delgado M.R., Nachtigall P., Thang H.V., Rubeš M., Bulánek R., Chlubná-Eliášová P.;
Measuring the Brønsted acid strength of zeolites ─ does it correlate with the O−H frequency shift probed by a weak base?
Physical Chemistry Chemical Physics, 2014, in press, doi: 10.1039/C3CP54738H

Abstract

The PhD thesis concerns the synthesis of novel zeolite materials, investigation of their properties and their possible use in catalytic application. The work was focused on the two-dimensional zeolites. The thesis was worked out at the Department of Synthesis and Catalysis at J. Heyrovský Institute of Physical Chemistry, AS CR.

Germanosilicate UTL (Si/Ge molar ratio 4.0-6.5) was found to undergo unique structural changes in the neutral or acid environment leading to transformation of its three-dimensional framework into two-dimensional layered material denoted IPC-1P. The UTL degradation, so called top-down synthesis, was enabled due to a presence of double-four-units (D4Rs), which can be seen as supporting units/pillars between the rigid layers. The preferential location of Ge in D4Rs makes the units an ideal target for their selective degradation. The interlayer space in lamellar IPC-1P was modified by swelling with long-organic chain surfactant (material IPC-1SW). To keep the interlayer space permanently expanded (up to 3.3 nm) the silica amorphous pillars were subsequently introduced (material IPC-1PI). The integrity of the layers and their preserved UTL character was confirmed in all members of IPC-1 family by HRTEM and electron diffraction measuring.

The layers of IPC-1P were condensed back and formed new zeolite structures. Depending on the chosen linkage, two novel zeolites were prepared, IPC-2 and IPC-4. The original D4R units in UTL were replaced by new single-four-ring (S4R) units in IPC-2 or by single Si-O-Si bridges in IPC-4. Three zeolites are closely related as they have the same UTL-like layers and differ only in the layer linkers. The size of their channel systems decreases with the size of the linkage between the layers in order UTL (14-12-ring) > IPC-2 (12-10-ring) > IPC-4 (10-8-ring). Zeolites IPC-2 and IPC-4 were verified by IZA Structure Commission as novel zeolites with three letter codes OKO (for COK-14, which is isostructure to IPC-2) and PCR (Prague Chemistry fouR), respectively.

The novel materials, IPC-1PI, IPC-2 and IPC-4, were prepared also with aluminium and they were tested for their catalytic activity in alkylation of toluene with isopropyl alcohol and the pillared Al-IPC-1PI in the reaction of styrene with phenol/*tert*-butylphenol.

The new approach for the synthesis of zeolites was designated the ADoR strategy: first the synthesis of the parent zeolite - Assembly, then its hydrolysis into layered material – Disassembly, followed by organisation of the layers and finally calcination into novel material – Reassembly. The mechanism of the ADoR was studied in detail under varying hydrolysis conditions.

The ADoR concept was successfully applied on other germanosilicate zeolite IWW. Its hydrolysis led to a lamellar material denoted IPC-5P. The layered IPC-5P was converted back to the three-dimensional structure by incorporation of silylating agent. Apart from the zeolite UTL and its IPC-1P, IPC-5P strongly tends to a formation of its original IWW framework. The 3D-2D-3D transformation of zeolite framework is a very unique case, which until now has not been described.

Abstrakt

Předložená disertační práce se zabývá syntézou nových typů zeolitů, jejich charakterizací a možným využitím v katalýze. Disertace byla zaměřena především na zeolity s dvourozměrnou strukturou. Práce byla vypracována na oddělení Syntézy a katalýzy na Ústavu fyzikální chemie J. Heyrovského AV ČR.

Germanokřemičitan UTL (s molárním poměrem Si/Ge 4.0–6.5) podléhá unikátním strukturním změnám, ke kterým dochází v neutrálním nebo mírně kyselém prostředí a které způsobují přeměnu jeho třírozměrné krystalické struktury na dvourozměrnou. Vzniklý vrstevnatý materiál byl nazván IPC-1P. Přeměna z třírozměrného na dvourozměrný zeolit, tzv. top-down syntéza, je umožněna díky přítomnosti stavebních jednotek tzv. double-four-ring (D4R), které tvoří pilíře mezi pevnými vrstvami daného zeolitu. D4R jednotky jsou přednostně tvořeny atomy germania a kyslíku a tvoří tak ideální cíl pro jejich selektivní odstranění. Mezivrstevný prostor u lamelárního IPC-1P bylo možno modifikovat interkalací činidla s dlouhým organickým řetězcem. Výsledný materiál byl označen IPC-1SW. Následně byly v meziprostoru vytvořeny pilíře z amorfního oxidu křemičitého, aby vrstvy zůstaly natrvalo oddáleny (až do vzdálenosti 3.3 nm). Materiál byl pojmenován jako IPC-1PI. U všech členů IPC-1 skupiny bylo potvrzeno zachování vrstev a jejich původní UTL struktura s použitím elektronové difrakce a HRTEM.

Vrstvy v IPC-1P bylo možné znovu spojit a tím připravit nové zeolitové struktury. V závislosti na délce vazby mezi vrstvami byly připraveny dva typy nových zeolitů, IPC-2 a IPC-4. Původní D4R jednotky v UTL byly nahrazeny novými single-four-ring (S4R) jednotkami u zeolitu IPC-2 nebo jednoduchými Si-O-Si vazbami u zeolitu IPC-4. Tyto tři zeolity jsou velmi blízké materiály, jelikož mají stejnou strukturu vrstev a liší se pouze v jejich propojení. Velikost kanálových systémů klesá s rozměrem spojek mezi vrstvami: UTL (14-12-četné kanály) > IPC-2 (12-10-četné kanály) > IPC-4 (10-8-četné kanály). IPC-2 a IPC-4 byly uznány Mezinárodní komisí IZA jako nové zeolity se zkratkou OKO (pro COK-14, který je isostrukturní s IPC-2) a PCR (Prague Chemistry fouR).

Nové typy materiálů, IPC-1PI, IPC-2 a IPC-4, byly připraveny také ve formě s hliníkem a byly testovány v alkylaci toluenu s isopropyl alkoholem a pilířovitý Al-IPC-1PI v reakci styrenu s fenolem/*tert*-butylfenolem.

Nový přístup pro přípravu zeolitů byl nazván ADoR, tzn. nejdříve je třeba zeolit připravit (Assembly), poté hydrolýzou převést na vrstvy (Disassembly), uspořádat vrstvy (organization) a nakonec kalcinací znovu spojit (Reassembly). Mechanismus ADoR byl detailně studován s použitím různých podmínek pro hydrolýzu.

Metoda ADoR byla úspěšně aplikována i na další germanokřemičitan, zeolit IWW. Jeho hydrolýzou byl připraven vrstevnatý materiál IPC-5P. Ten byl zpětně převeden do třírozměrné struktury pomocí interkalace silylačního činidla. Na rozdíl od zeolitu UTL a jeho IPC-1P u materiálu IPC-5P byla zjištěna silná tendence formovat původní IWW strukturu. Tato jedinečná 3D-2D-3D přeměna zeolitové struktury je ojedinělým případem, který do současné doby nebyl popsán.

Content

1 Aims of the study

The PhD thesis deals with the synthesis of novel zeolitic materials and investigation of their properties. The work is focused on two-dimensional zeolites and a new approach for their synthesis, so called top-down synthesis. The main objectives are summarized as follows:

- Synthesis of novel zeolitic materials using top-down approach.
- Characterization of novel materials using different techniques like X-ray powder diffraction, nitrogen and argon adsorption measurement, microscopy techniques (scanning and transmission electron microscopy), chemical analysis and Fourier transform infrared spectroscopy (FTIR) using different probe molecules to investigate the acidity of prepared materials.
- Interpretation of the characteristics with respect to different structural parameters of novel prepared materials.
- Testing of new materials for catalytic activity (e.g. in toluene alkylation with isopropyl alcohol) and comparing the results with commercially used zeolites, e.g. BEA, MFI.

2 Introduction

2.1 Molecular sieves and zeolites

Molecular sieves are a large group of porous materials with a wide range of applications in adsorption[1], catalysis[2,3,4], sensing[5], fuel cells[6], etc. They can be crystalline or amorphous materials with various chemical compositions. Molecular sieves include for instance: zeolites, mesopore materials, activated carbon, phosphates, arsenates or nitrides. Zeolites are an important class of molecular sieves. They are microporous aluminosilicates with a regular three-dimensional framework. Zeolites are environmentally friendly materials and can be of natural or synthetic character. At present, there are 213 known structural types[7]. The primary building units are tetrahedra of SiO_4 and AlO_4 (for simplicity, Si or Al are designated as T atoms). Individual tetrahedra can be connected by oxygen bridges through their corners, never edges or planes. Connecting primary building units can create so called secondary building units like three-, four-, six rings, double four- and six rings, etc. By combining secondary building units a three-dimensional channel structure is formed.

Zeolite frameworks possess pores and cavities of molecular dimensions (less than 2 nm). The size of channel system entrance is determined by the number of T atoms (T = 7, 8, 9, 10, 12, 14, etc.). According to the size of entrance windows zeolites are divided into four groups:

I. small-pore zeolites (8-rings with pore dimensions up to 0.4 nm, e.g. LTA, CHA);
II. medium-pore zeolites (10-rings with pore dimensions up to 0.55 nm, e.g. MFI, MWW);
III. large-pore zeolites (12-rings with pore dimensions up to 0.75 nm, e.g. FAU, BEA);
IV. extra-large-pore zeolites (14-rings and more with pore dimensions around 1 nm, e.g. UTL, CFI).

The individual channel systems can be of different sizes. Zeolites with independent and non-intersecting channels have a one-dimensional channel system (e.g. LTL, CFI). Zeolites with channels intersecting in two and three dimensions have two-dimensional and three-dimensional channel systems with channels of the same or different sizes (e.g. FER, UTL have a two-dimensional system and BEA, FAU have a three-dimensional channel system). Large cavities may be created at channel intersections. The size and shape of the channel system are one of the most important characteristics of zeolites involving in the effect called shape-selectivity[8].

The shape selectivity is based on the relationship between the kinetic diameter of organic molecules and the size of zeolite channels. Three different types of shape-selectivity are

distinguished (**Fig. 1**): I. *reactant selectivity* - only molecules of certain size and shape can penetrate into the channel system; II. *product selectivity* - the formed products are too bulky to diffuse out and they can block the catalyst channels or can be converted to smaller molecules and leave the channels; III. *restricted transition-state selectivity* - only intermediates, which fit into the channels or cavities can be formed during the reaction.

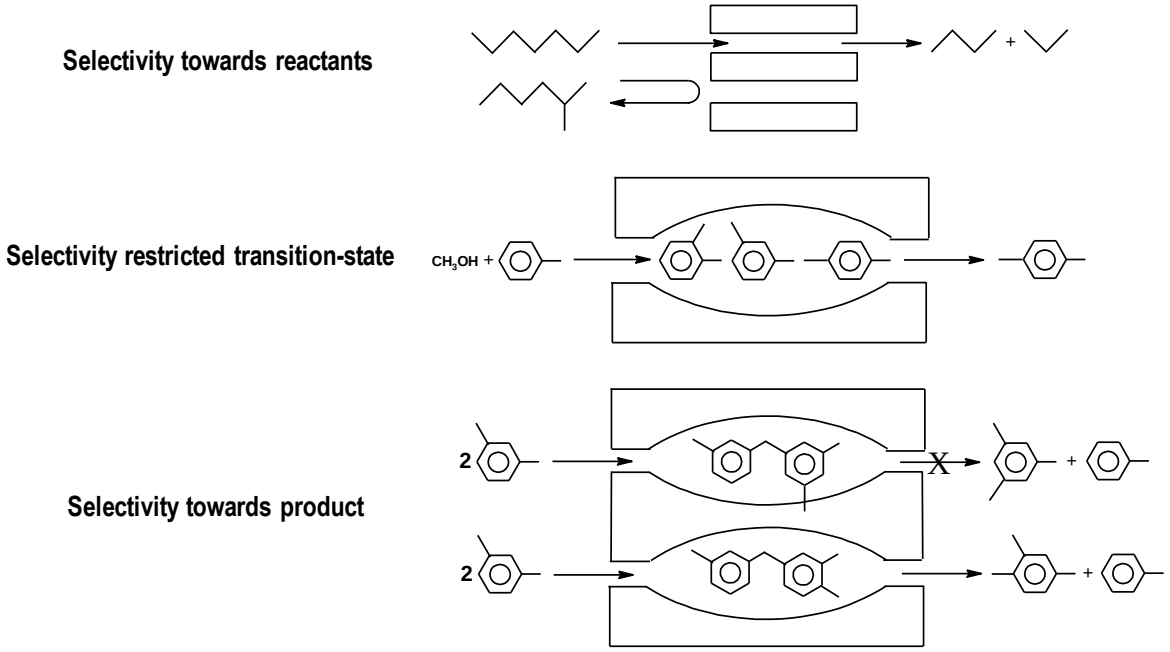

Fig. 1 Different types of shape selectivity products.

Generally, the chemical composition of zeolites can be described by the following formula $\mathbf{M_{x/n}[(AlO_2)_x(SiO_2)_y].wH_2O}$. M means the exchangeable cation, *n* the cation valence, *y*/*x* is silicon to aluminium molar ratio (Si/Al) and *w* the number of water molecules per unit cell[9].

Zeolites are aluminosilicates and consequently the total charge of the framework is negative and it is balanced by extra-framework cations like H^+, NH_4^+, Na^+, K^+, Ca^{2+}, etc. Silicon in the framework can be substituted with cations of similar size and the same charge, e.g. Ti^{4+}, Ge^{4+}, etc., or by cations of different size and charge, e.g. B^{3+}, Fe^{3+}, Ga^{3+} and others. The important attribute of zeolites is their acidity, which depends on the nature of heteroatom. Acid centres can have Brønsted or Lewis character (**Fig. 2**). Their concentration, strength and location can be determined by FTIR spectroscopy using adsorption of various probe molecules (e.g. pyridine, acetonitrile).

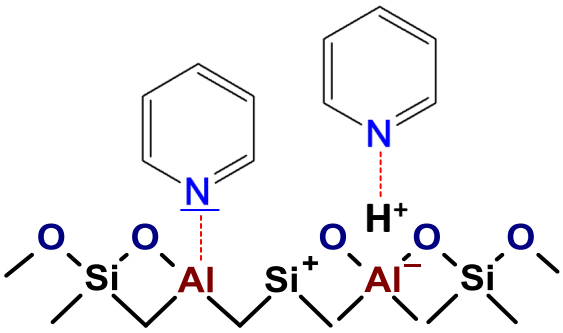

Fig. 2 Schematic view on the Lewis (left) and Brønsted types (right) of acid centres in the interaction with pyridine molecules.

The first laboratory synthesis of zeolites was performed by Richard Barrer and Robert Milton in late 1940s[10] preparing zeolites A, X and Y in a pure inorganic environment[11,12,13]. Later, inorganic components were partially replaced by organic cations like quaternary ammonium salts[14,15]. Using so-called organic structure directing agents (SDAs) led to the preparation of high silica zeolites, which are hydrothermally more stable.

Traditionally, zeolites can be synthesized in aqueous media (usually in a basic environment) under hydrothermal conditions (temperature 100 - 200 ˚C) and autogeneous pressure. The reaction mixture contains a source of silicon (e.g. tetraethyl orthosilicate or silica in different forms like Cab-O-Sil M5 etc.), aluminium (e.g. aluminium nitrite, aluminium hydroxide or oxide), and/or other heteroatoms (e.g. boron, gallium, titanium in their compounds), inorganic ions (e.g. sodium hydroxide, potassium hydroxide) and/or organic ions (SDA like quaternary ammonium salts) and a solvent (usually water). The size, geometry, rigidity, and hydrophobicity of the SDA are very important features determining its ability to form zeolite structures. However, the relation between the shape and size of the SDA and shape and size of the zeolite channels has not been fully explained yet.

Overall, zeolites possess many exceptional properties and advantages in comparison with other crystalline materials, which can be summarized as follows[16,17]:

- well-defined crystalline porous structure with variable dimension and geometry of porous system
- high hydrothermal stability
- high internal volumes providing surface areas up to 600 m^2/g
- narrow range of pore size distribution in each zeolite
- possibility of tuning chemical and textural properties through isomorphous substitution or various post-synthesis modifications
- shape-selectivity properties related to the ratio between kinetic diameters of organic molecules and the size of the zeolite channels
- environmentally friendly materials.

2.2 3D and 2D zeolites and their post-synthesis modifications

Zeolites have been traditionally found and synthesized in complete three-dimensional (3D) four-connected framework forms[18,19]. When the third dimension is limited to 2-3 nm (corresponding to 1-2 unit cells) the material is termed a two-dimensional (2D) or layered/lamellar zeolite. Usually upon calcination the three-dimensional framework is formed again through the condensation of the silanol groups present on the layer surface.

In the three-dimensional zeolite the presence of micropores with pore openings of less than 1 nm is often connected with diffusion limitations that adversely affect catalytic activity[20,21,22]. Reactants and products with sizes beyond the pore dimensions cannot diffuse into or out of zeolite crystals. Reduction of the zeolite crystal thickness can reduce diffusion path lengths. Thus, the lamellar zeolitic materials can overcome the problems with molecular diffusion. To date, ten different zeolite frameworks have been recognized to crystallize as layered precursors[23]: MWW[24,25], NSI[26], FER[27], SOD[28], CAS[29], RWR[30], RRO[31], AFO[32], CDO[33,34] and MFI[35,36].

Great advantage of layered zeolites is the possibility to manipulate with the layers before calcination. The most outstanding example is the layered precursor MCM-22P (with one unit cell thickness, 2.5 nm) from the MWW family, on which the rich chemistry of lamellar zeolites will be demonstrated. The scheme in **Fig. 3** summarizes all different forms of zeolites in the MWW family.

The layers of MWW in MCM-22P zeolite are not connected by covalent bonding but by hydrogen bonding and some molecules of organic SDA (namely hexamethylenimine) are located between the layers. The interlayer space in the as-made MCM-22P can be expanded by swelling with cationic surfactant solutions (e.g. hexadecyltrimethylammonium)[37,38]. The long organic chains are stacked approximately perpendicular to the layers and keep the layers separated. However, after calcination the organic molecules are removed and the layers contract back. To achieve permanent separation of the layers the swollen MCM-22P is subsequently pillared by the addition of inorganic pillars from amorphous silica. Hybrid MCM-36 material combines micro- and mesopores[39]. The swollen precursor MCM-22P can be also delaminated by sonication obtaining material ITQ-2[40].

The three-dimensional framework of MWW can be formed either by calcination of layered MCM-22P precursor or by direct synthesis as so called MCM-49. Zeolites MCM-22 and MCM-49 are isostructural and differ mainly in the composition. When hexamethyleneimine is used as a structure directing agent, MCM-49 generally has a lower Si/Al molar ratio (<11) than MCM-22P does (>11)[25]. A factor that influences the formation of either MCM-22P or MCM-49 is the molar ratio of the organic cation R_o (SDA) to the inorganic cations R_i (e.g. Na, K, or Rb). When the ratio R_o/R_i is typically less than 2.0, the formation of MCM-49 is favoured[25]. Apart from MCM-22 zeolite, MCM-49 crystallizes through its delaminated intermediate designated as MCM-56[41] (**Fig. 3**).

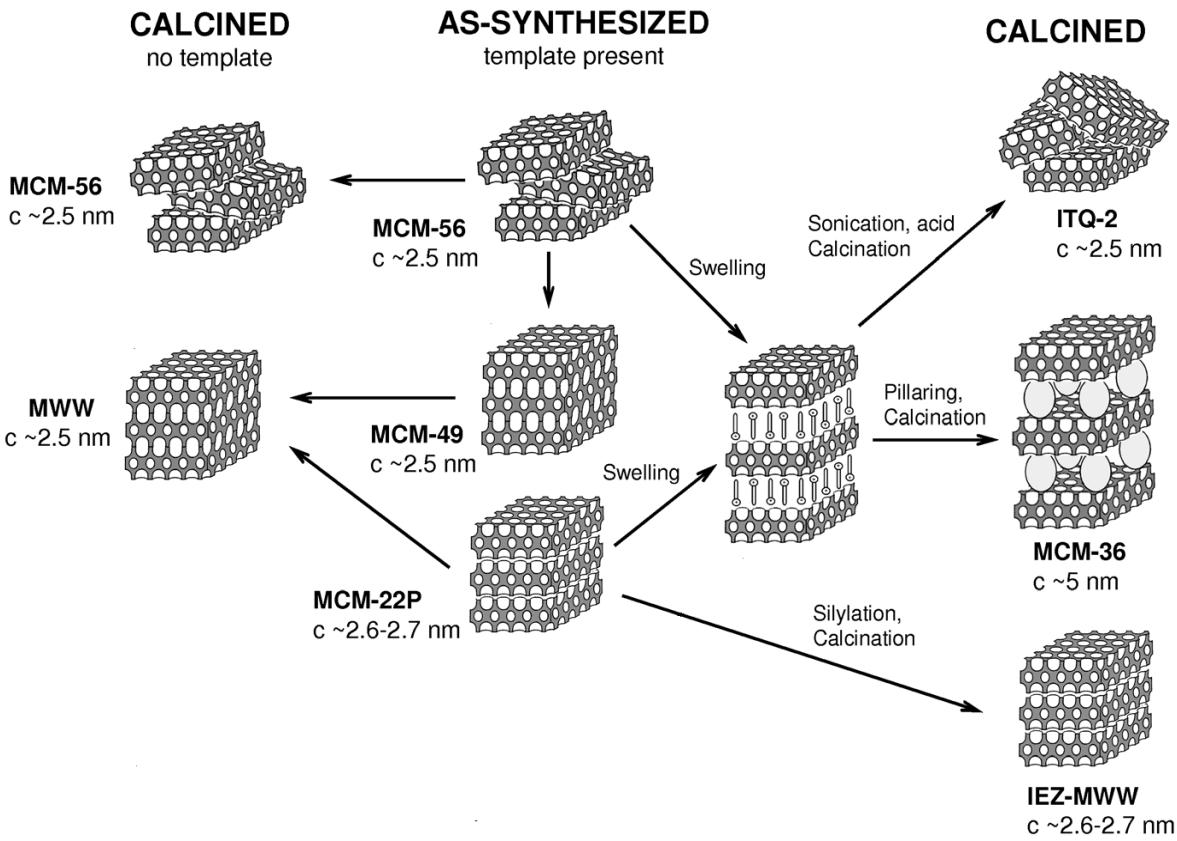

Fig. 3 The scheme of zeolites from MWW family illustrating proposed layer arrangements and post-synthesis pathways[39].

The MCM-22P layers can be also reconnected via new silicate bridges by the procedure called *stabilization*[42]. Different silylating agents like diethoxydimethylsilane create new connections between the layers. The surface silanol groups react with dialkoxysilanes and build new bridges. So called Interlamellar Expanded Zeolite, IEZ-MWW, possesses novel structure with enlarged pore windows (12-ring) in comparison to normal MCM-22 (10-ring, **Fig. 4**)[42]. However, IEZ-MWW cannot be considered as a new zeolite based on the basic definition of a zeolite, which states that a zeolite has a regular three-dimensional framework with silica or aluminium tetrahedra connected in three directions. The new silica bridges between the MWW layers are not fully connected in all three directions, and thus IEZ-MWW presents a novel zeolitic material but not a new zeolite framework.

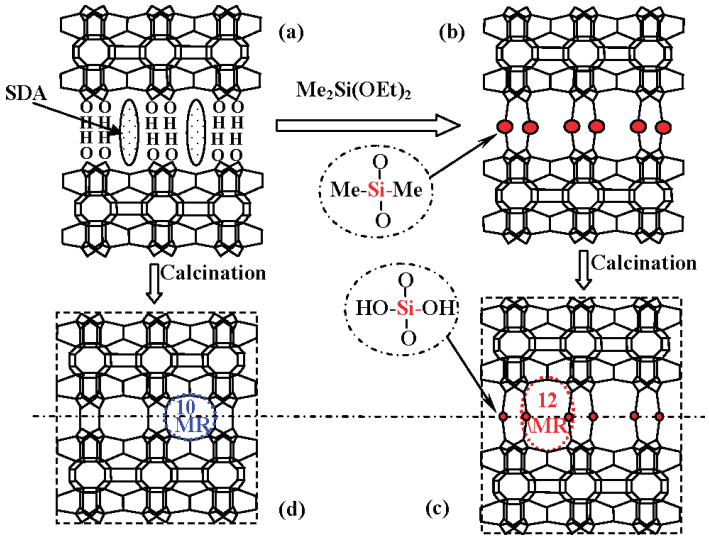

Fig. 4 Schematic view on layered MCM-22P with the organic SDA between the layers **(a)**, the layers after one-step dialkoxysilylation **(b)**, followed by calcination to remove organic moieties **(c)**. View on the common three-dimensional structure of MWW obtained by direct calcination of the layered MCM-22P **(d)**[42].

2.3 Zeolite UTL

Germanosilicate zeolite UTL belongs to the extra-large pore zeolites and it was first synthesized independently by two research groups - in Spain (denoted ITQ-15[43]) and in France (denoted IM-12[44]). 14- and 12-ring intersecting channels form a two-dimensional channel system with pore sizes of 0.85 x 0.55 nm and 0.95 x 0.71 nm[7,45], respectively (**Fig. 5**).

Generally, germanium is known to stabilize the formation of D4Rs and to be preferentially located in them[46,47,48,]. The mean value of Si-O-Si bond in zeolitic frameworks is 154 ± 9° while for Ge-O-Ge it is about 130°[49]. The presence of germanium increases the probability of forming zeolite frameworks with D4Rs or D3Rs due to the smaller Ge-O-Ge angle compared with larger Si-O-Si angle[46]. In zeolite UTL, D4Rs connect mostly pure silica layers, which contain primarily 5-rings. The layers themselves consist of chains of [$4^1 5^8$] units and the chains are linked to one another via one or two additional tetrahedra (**Fig. 5**).

Germanosilicate UTL can be prepared with various spiroazocompounds as organic structure directing agents (SDAs). The common by-products in the synthesis are the dense-phase of βGeO_2 and zeolites STF and ITE. Thirteen organic SDAs were found to preferentially form UTL structure (**Fig. 6**)[50]. They differ in the structure, hydrophilicity/hydrophobicity balance, rigidity and p*K*a. The optimum synthesis time was determined to be 3-7 days at a Si/Ge molar ratio of 2 and (Si+Ge)/SDA molar ratio from 1.7 to 6. It was found a connection between the template nature, the synthesis time and the final UTL properties (porosity, crystallinity, shape and size of the crystals, etc.)[50].

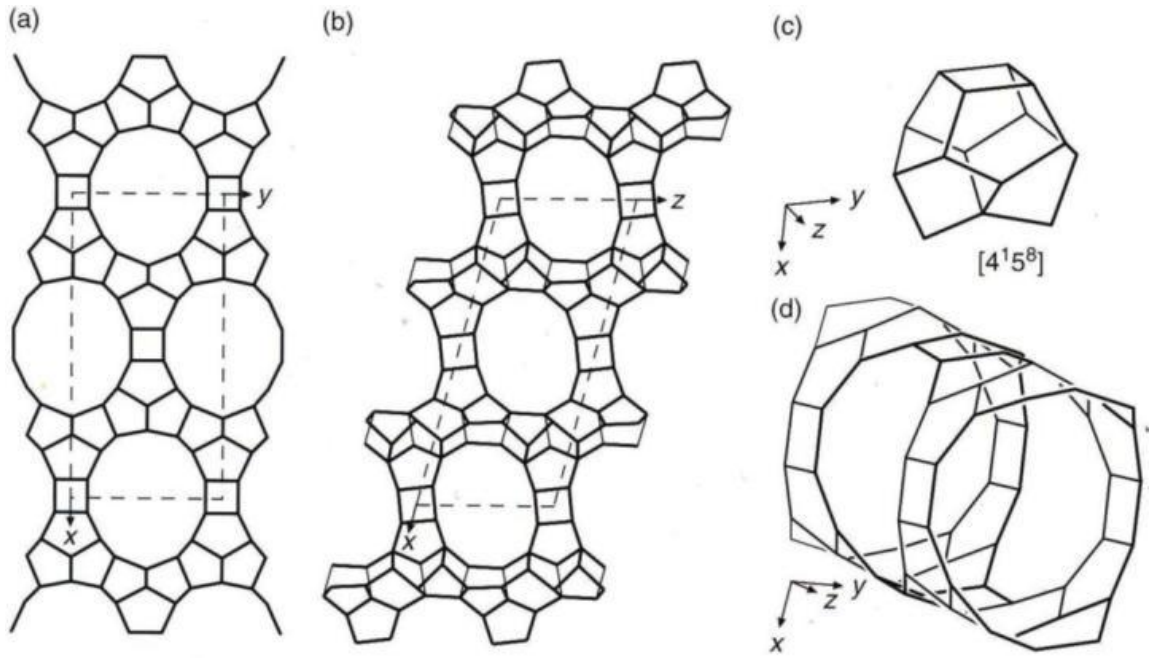

Fig. 5 The UTL framework type. Projection **(a)** down the *z* axis, and **(b)** down the *y* axis. **(c)** The [$4^1 5^8$] cage found in the layers. **(d)** The intersection of 14- and 12-ring channels.

Although UTL has not been yet prepared as a pure silicate or aluminosilicate, it can be isomorphously substituted with different three-valent heteroatoms (boron, aluminium, iron, gallium, and indium)[51]. The presence of heteroatoms in the reaction mixture significantly influences the pH borders acceptable for the synthesis of pure UTL phase. The maximum concentration of heteroatoms in UTL was found 1.5 mol % for Al and Ga, 6 mol % for In and 13 mol % for B. In the case of Fe-UTL, iron oxide was found to form another phase. Thus, the upper concentration limit for Fe in UTL was not determined. It was found that the presence of heteroatom influences the size of UTL crystals, which decreases in the order Al > In > Ga > Fe ≈ B[51].

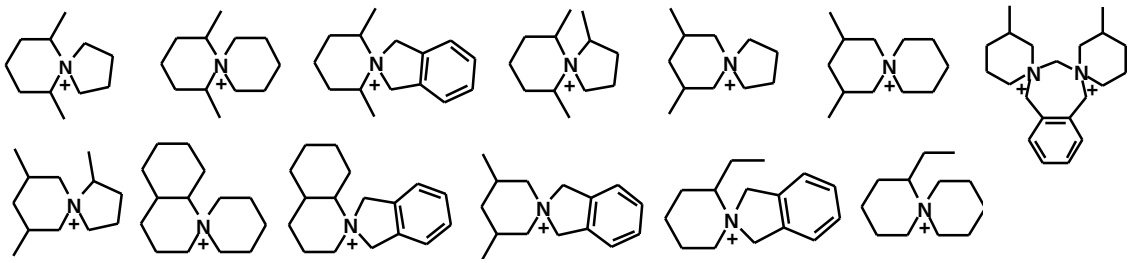

Fig. 6 The organic structure directing agents for preferential formation of UTL phase [50].

As it was mentioned above, UTL cannot be directly prepared as pure silica zeolite. However, recently Wu and co-workers published a post-synthesis modification of some germanosilicates leading to highly siliceous zeolites[52]. The germanosilicates with UTL, UWY, BEC and IWR topology are known to be less hydrothermally stable. In the stabilization process Ge atoms in D4R units were replaced by Si atoms, which further

stabilized the structure without degradation of the parent germanosilicate framework. Using the novel post-synthesis approach UTL was prepared with Si/Ge ratio 233[52].

Extra-large pore zeolite UTL (substituted with B, Al, Ga, Fe) was tested for its catalytic activity in different reactions like acylation of *p*-xylene with benzoyl chloride[53], Beckmann rearrangement of 1-indanone oxime[53], disproportionation of toluene[54], toluene alkylation with isopropyl alcohol[54], and trimethylbenzene disproportionation/isomerisation[54].

2.4 Zeolite IWW

Zeolite IWW was first prepared as a pure germanosilicate ITQ-22 and substituted with aluminium[55]. Its structure contains [$4^4 5^8 6^{12}$] cages that are stacked along the *c* axis, forming D4R units and giving rise to columns (**Fig. 7**). Each column is linked to the nearest ones either directly or through an additional bridging T atom. IWW structure contains fully interconnected 8-10-12-ring channel system with pore sizes of 0.33 x 0.46 nm, 0.49 x 0.49 nm, 0.6 x 0.67 nm, respectively[7]. The 12- and 8-ring channels run parallel to the *c* axis, and they are both intersected by a sinusoidal 10-ring channel centred at the D4R units.

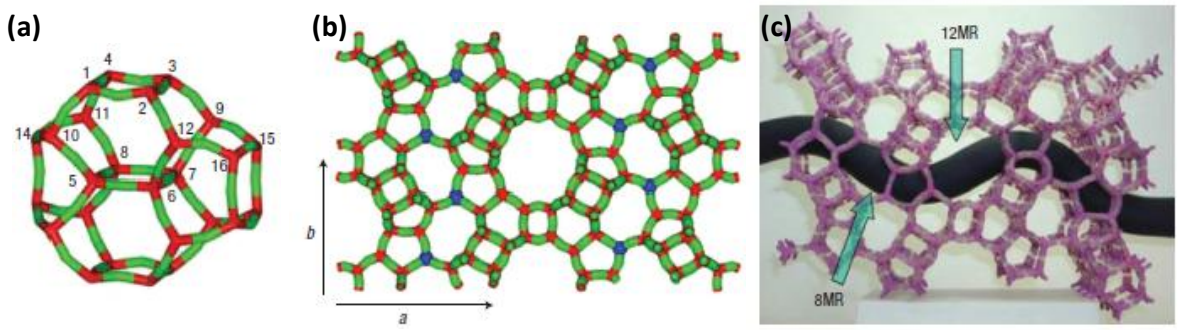

Fig. 7 Structure of IWW. **(a)** [$4^4 5^8 6^{12}$] cage, red T atoms, green oxygen atoms. **(b)** framework viewed along c axis (red T atoms, green oxygen atoms, blue bridge atoms). **(c)** three-dimensional structure model showing 8- and 12-ring channels that are intersected by sinusoidal 10-ring channel showed as a black ribbon[55].

3 Experimental part

3.1 Synthesis and modification of UTL

3.1.1 Zeolite UTL and its hydrolysis

Structure directing agent (SDA) for the synthesis of UTL, (6*R*,10*S*)-6,10-dimethyl-5-azoniaspiro[4,5] decane hydroxide, was prepared according to the literature[50]. To the water solution (140 ml) of sodium hydroxide (5.68g) and 1,4-dibromobutane (30.66g) the amount of (2*R*,6*S*)-2,6-dimethylpiperidine (16.07g) was added drop-wise and the mixture was refluxed under intensive stirring for 12 hours. After cooling in an ice bath an ice-cooled 50% (wt) solution of NaOH (70 ml) was added and further the solid NaOH was adding until the oil product was formed. After crystallization the solid was filtered and extracted with chloroform. The organic fraction was dried using anhydrous sodium sulfate and partially evaporated. The ammonium salt was washed out with diethyl ether. The obtained template was ion-exchanged into hydroxide form using AG 1-X8 Resin (Bio-Rad).

Zeolite UTL was prepared by procedures published in details in Ref. [50,51,56,57]. A typical reaction mixture had the molar composition of the gel: 0.6–1.0 SiO_2: 0.6–0.2 GeO_2: 0.3–0.7 SDA: 30–33 H_2O. The gel was prepared by dissolving of amorphous germanium oxide in the solution of SDA. Then, silica (Cab-O-Sil M5) was added to the solution and the mixture was stirred at ambient temperature for 30 min. The resulting gel was charged into Teflon-lined steel autoclave and heated at 175 °C for 3–9 days. The solid product was recovered by filtration, washed out with distilled water and dried at 60 °C. The as-synthesized zeolite was calcined in a stream of air at 550 °C for 6 hours with a temperature ramp of 1 °C/min.

Calcined UTL was hydrolysed in acid solutions. Different acid solutions of various concentrations were used - hydrochloric acid (0.01-12M), acetic acid (0.1-12M) or nitric acid (0.1-1M). Typically, calcined UTL was stirred with 0.1M HCl solution (ratio 1g/250ml) at 85-100 ˚C for 16-24 hours. The product was separated by filtration, washed out with water and dried at 65 ˚C. The hydrolysed material was denoted IPC-1P. A part of it was further calcined at 550 ˚C for 6 hours and denoted IPC-1.

3.1.2 Intercalation chemistry of IPC-1P

Swelling

Hexadecyltrimethylammonium cation (C_{16}TMA) was used as a typical swelling agent. It was used as a mixture of C_{16}TMA-Cl (25 wt.% water solution) with tetrapropylammonium hydroxide (TPA-OH, 40 wt.% water solution) or C_{16}TMA-Cl was ion-exchanged into hydroxide form with AG 1-X8 resin (Bio-Rad). The IPC-1P was stirred with a mixture of C_{16}TMA-Cl and TPA-OH (in the ratio for 1g of IPC-1P, 27g of C_{16}TMA-Cl and 3g of

TPA-OH) or with C_{16}TMA-OH solution (in the ratio for 1g of IPC-1P 20ml of C_{16}TMA-OH) at ambient temperature for 16-24 hours. The solid was separated and washed with water by series of centrifugation and decantation. The swollen material was denoted IPC-1SW. A part of the material was further calcined at 550 ˚C for 6 hours and denoted IPC-1SW calc.

Pillaring

The swollen material IPC-1SW was pillared with tetraethyl orthosilicate (TEOS, ratio 1g/50ml). The slurry was stirred at 85 ˚C for 16 hours. After cooling down the product was separated by centrifugation and dried at ambient temperature. In the following step, the pillared material was hydrolysed in the open beaker with water (ratio 1g/100ml) at ambient temperature for 16 hours. After filtration and drying, the product was calcined at 550 ˚C for 6 hours. The pillared material was denoted IPC-1PI.

Stabilization

For stabilization different alkoxysilylating agents can be used, e.g. diethoxydimethylsilane, triethoxymethylsilane, tetraethoxysilane. Typically, diethoxydimethylsilane (DEDMS) was mixed with IPC-1P in 1M HNO_3 solution (ratio 1g of zeolite/0.1g DEDMS/10g 1M HNO_3). The reaction was performed in the Teflon-lined autoclave at 175 ˚C for 16 hours. The product was after filtration and drying calcined at 550-750 ˚C for 6 hours. The final zeolite was denoted IPC-2.

Intercalation of organic amines

For intercalation of IPC-1P layers various organic amines, e.g. octylamine, or ammonium salts, e.g. tetramethylammonium cation, tetrapropylammonium cation, were used. Typically, IPC-1P was stirred with octylamine (in the ratio 1g/65ml) at 70 ˚C for 16 hours. The intercalated material was separated by centrifugation, dried at 40˚C and finally calcined at 550-750 ˚C for 6 hours to obtain zeolite IPC-4.

3.1.3 Synthesis of zeolite IWW and its post-synthesis modifications

Zeolite IWW was synthesized according to the procedure described in the literature[55]. The typical reaction mixture has the molar composition 0.66 SiO_2: 0.33-1 GeO_2: 0.25 SDA: 3.5 H_2O, where 1,5-bis-(*N*-methylpyrrolidinium)pentane was used as a structure directing agent (SDA). The gel was prepared by dissolving of GeO_2 in the solution of SDA (in hydroxide form), then tetraethyl orthosilicate as a source of silica was added. The gel was stirred for 30 minutes and then charged into Teflon-lined steel autoclaves. The synthesis proceeded under agitation at 175 ˚C for 10 days. The product was filtered, washed with water, dried and calcined at 550 ˚C for 6 hours.

The calcined zeolite was treated in various acid solutions in the same way as zeolite UTL (for details see **Chapter 4.4.1**). The same post-synthesis modifications described for IPC-1P were applied on hydrolysed IWW, which was designated IPC-5P.

3.2 Catalytic experiments

Zeolites Al-MFI and Al-BEA used as standard catalysts were purchased from Zeolyst and used after four-times repeated ion-exchange with 0.5M NH_4NO_3 solution.

Toluene alkylation

The catalytic behaviour of novel zeolites was tested in toluene alkylation with isopropyl alcohol and compared with the conventional Al-MFI and Al-BEA zeolite. The reaction was investigated in a down-flow glass micro-reactor with a fixed bed of catalyst under atmospheric pressure. Before the catalytic run, zeolite catalysts were activated at 500 °C in nitrogen stream for 120 min. The alkylation of toluene was performed at 250 °C with toluene to isopropyl alcohol (Tol/*i*-PrOH) molar ratio of 9.6 and WHSV based on toluene equal to 10 h^{-1}. The reaction products were analyzed using an "on-line" gas chromatograph (Agilent 6890 Plus) with flame ionization detector and a high-resolution capillary column. The first analysis was performed after 15 min of time-on-stream (T-O-S) and the other followed in approx. 55 min interval.

Hydroarylation of styrene

Hydroarylation of styrene with phenol or *tert*-butylphenol was investigated in a liquid phase under atmospheric pressure at the reaction temperature of 75 °C in a multi-experimental work station StarFish (Radleys Discovery Technologies UK). The reactions were performed in a 25 ml round bottom flask equipped with a condenser. In a typical experiment, 1 mmol of styrene, 2 mmol of phenol or *tert*-butylphenol, 0.2 g of dodecane (internal standard), 0.2 g of catalyst and 10 ml of cyclohexane (solvent) were used. The catalysts were activated by heating at 450 °C for 90 min with a temperature rate 10 °C/min. The catalyst was added into the heat up mixture of reactants as the last one.

3.3 Characterization techniques

The structure and crystallinity of zeolites were determined by X-ray powder diffraction using Bruker AXS D8 Advance diffractometer equipped with a graphite monochromator and a position sensitive detector Våntec-1 using CuKα radiation in Bragg–Brentano geometry.

Adsorption isotherms of nitrogen (at -196 °C) and argon (at -186 °C) were measured on a Micromeritics ASAP 2020 static volumetric instrument. In order to attain sufficient accuracy in the accumulation of the adsorption data, the ASAP 2020 was equipped with pressure transducers covering the 133 Pa, 1.33 kPa and 133 kPa ranges. Prior to the

sorption experiments, samples were outgassed at 110 °C under turbomolecular pump vacuum until the residual pressure of 0.5 Pa was obtained. After further heating at 110 °C for 1 h the temperature was increased (1 °C/min) until the temperature 300 °C was achieved. This temperature was maintained for 6 h.

The surface area (S_{BET}) was evaluated by BET method[58] using adsorption data in the p/p_0 range of 0.05-0.20. The adsorbed amount at relative pressure $p/p_0 = 0.98$ reflects the total adsorption capacity (V_{tot}). For adsorption isotherms of nitrogen, the *t*-plot method[59] was applied to determine the volume of micropores (V_{mic}). For adsorption isotherms of argon, the NLDFT algorithm (using standard Micromeritics software for cylindrical pores for Argon on Oxides at -186 °C) was used to calculate the volume of micropores (V_{mic}) and pore-size distribution for pores less than 5 nm in diameter. The volume and pore-size distribution of mesopores with the size from 5 to 20 nm was calculated from the desorption branch of the isotherm using BJH method[60] with Halsey equation.

The concentration and the type of acid sites were determined by adsorption of acetonitrile as a probe molecule followed by FTIR spectroscopy (Nicolet 6700 FTIR with DTGS detector) using the self-supported wafer technique. Prior to adsorption of probe molecules, self-supported wafers of zeolite samples were activated in-situ by overnight evacuation at temperature 450 °C. CD_3CN adsorption proceeded at room temperature for 30 min at equilibrium pressure 5 Torr, followed by 30 min degassing at room temperature. To obtain quantitative analysis the molar absorption coefficients for CD_3CN adsorbed on Brønsted acid sites (ν(C≡N)-B at 2297 cm^{-1}, ε(B) = 2.05 ± 0.1 cm μmol^{-1}) and strong and weak Lewis acid sites (ν(C≡N)-L_1 at 2325 cm^{-1} ν(CN)-L_2 2310 cm^{-1}, ε(L) = 3.6 ± 0.2 cm μmol^{-1}) were used[61]. Integral intensities of individual bands were used and spectra were normalized to the wafer thickness 10 mg cm^{-2}.

The size and shape of zeolite crystals were examined by scanning electron microscopy (SEM, Jeol, JSM-5500LV). For the measurement, crystals were coated with a thin platinum layer by sputtering in vacuum chamber of a BAL-TEC SCD-050.

Theoretical calculations and simulations of XDR patterns and modelling of zeolites in IPC-1 family (IPC-1P, IPC-2, IPC-4) and IPC-5 were performed by the group of Assoc. Prof. Petr Nachtigall at the Faculty of Natural Sciences, Charles University (Czech Republic).

The microstructures of zeolites were investigated using high resolution transmission electron microscopy (HRTEM) on a Jeol JEM-2011 electron microscope operating at an accelerating voltage of 200 kV. The measurements were performed by the group of Prof. Wuzong Zhou at St. Andrews University (United Kingdom).

The chemical analysis was obtained by the Energy Dispersive X-Ray Spectroscopy (EDX) on a Jeol JSM 5600 instrument at St. Andrews University (United Kingdom).

For the structure analysis of IWW powder diffraction data were collected on the Materials Science-Powder X04SA Beamline at the Swiss Light Source (SLS) at Paul Scherrer Institut in Villigen (Switzerland)[62].

Solid-state NMR spectra were acquired using Bruker Avance III 600 MHz spectrometer equipped with a widebore 14.1 T magnet. Powdered samples were packed into conventional 4 mm ZrO_2 rotors. ^{29}Si MAS NMR spectra were obtained using single-pulse experiments, with a recycle interval of 180 s. The MAS rate was 10 kHz. For the ^{27}Al MAS NMR the MAS rate of 14 kHz was used. The measurements were performed at St. Andrews University (United Kingdom).

4 Results and Discussion

4.1 Zeolite UTL and its transformation into lamellar material

Zeolite UTL was synthesized as germanosilicate with Si/Ge molar ratio in the range 4.0-6.5 and was also prepared with boron, aluminium, and other three-valent elements. UTL was found to have a unique ability to undergo structural changes in neutral or acid environment resulting in its transformation into layered material. This attribute is closely related to its unique structure characterized by almost pure silica solid layers connected with double-four-ring units (D4R) preferentially occupied by germanium. Hence, D4Rs are considered not only as the connecting units but also as centres of instability due to the presence of germanium. The bonds Ge-O-Ge in the D4Rs are less stable then Si-O-Si in the layers and therefore they are predisposed to selective breaking (**Scheme 1**).

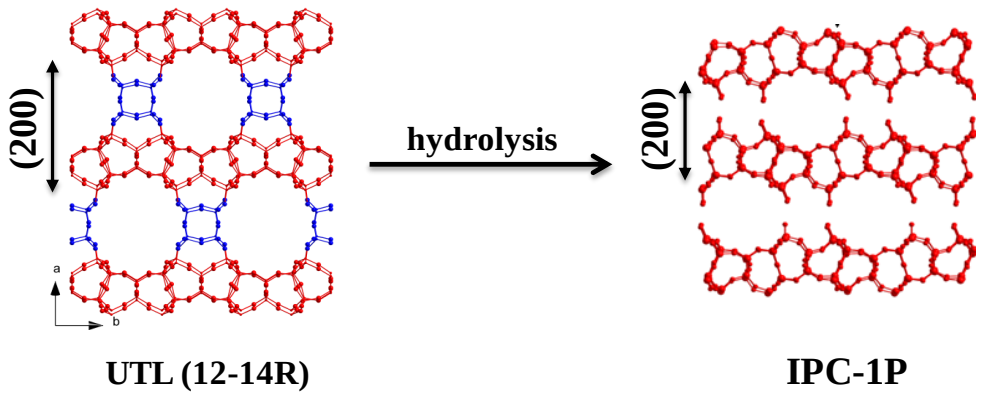

Scheme 1 A schematic view on the 3D to 2D transformation of zeolite UTL into layered IPC-1P. The 'layers' in the 3D UTL structure (left) are shown in red and D4R units (occupied mainly with germanium) that connect the layers are shown in blue.

Fig. 8 shows the comparison of the X-ray powder diffraction (XRD) pattern of calcined zeolite UTL and its hydrolysed form (using 0.1M HCl at 85 ˚C for 16 hours), which was designated IPC-1P (**I**nstitute of **P**hysical **C**hemistry, **P** for layered precursor). The pattern is significantly changed consisting of one dominant reflection and lower intensity diffraction lines. The (200) reflection in UTL reflects the half of the unit cell size along the axis *a* (**Scheme 1**). Removing of D4Rs causes structural changes and change of the unit cell size with an unequivocal shift of (200) reflection to the higher 2θ values evidencing the decrease in the interlayer distance. The original position of (200) in UTL is 6.15˚ (2θ) and after hydrolysis it is shifted up to 8.45˚ (2θ) proving the interlayer contraction about 0.4 nm after removing of all D4Rs (calculated from (200) peak positions and corresponding d-spacing values).

Generally, for transformation of three-dimensional UTL into layered IPC-1P water or low concentrated acid solutions like 0.01-1M HCl, CH_3COOH or HNO_3 at temperatures 85-

100 ˚C can be used. The full separation of the layers in IPC-1P is indicated by the presence of dominant (200) peak in the range 8.3-8.5˚ (2θ).

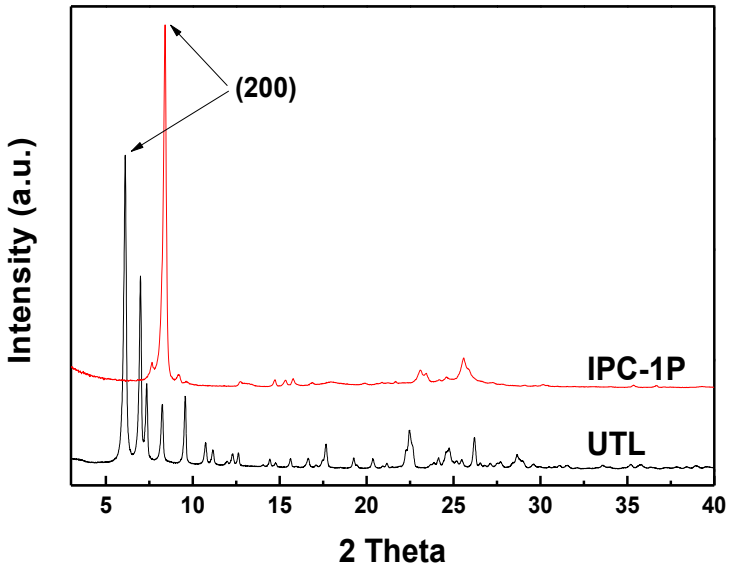

Fig. 8 XRD patterns of calcined UTL zeolite and after hydrolysis in 0.1M HCl at 85 ˚C for 24 hours. The arrows mark the positions of the interlayer reflection (200).

4.1.1 New two-dimensional zeolites of IPC-1 family

The manipulation with the two-dimensional ultra-thin zeolitic layers is a useful tool to achieve the expansion of the interlayer space and increase in the accessibility to catalytic active centres, as it was discussed in **Chapter 2.2**. The same principles demonstrated on MWW family were applied on the novel layered material, IPC-1P. The structural and textural changes during the treatments will be shown and discussed on the representative group of samples, denoted as IPC-1 family. The individual samples undergoing the same treatments (like swelling and pillaring) can slightly differ in the position of the interlayer peak in XRD patterns or/and in the surface areas and pore volumes, however, the general trend in all cases remains.

The layered IPC-1P was intercalated with an organic surfactant with long-hydrophobic chain and one ammonium group on the end, hexadecyltrimethylammonium cation ($C_{16}TMA^+$). The organic surfactant can be used in its hydroxide form or as chloride or bromide but in the mixture with tetrapropylammonium hydroxide solution. The basic source cleaves the interlayer linkage of hydrogen bonds while SiO^- groups on the layer surface repulse each other and provide enough space for intercalation of long-chain surfactant. The molecules of surfactant stacked approximately perpendicular between the layers of IPC-1P and thus expand the interlayer space (**Scheme 2**). The swollen material, designated as IPC-1SW, shows the XRD pattern dominated by low angle peaks (**Fig. 9**). The d-spacing of the first most intensive peak at 2.6˚ (2θ) is equal to 3.4 nm corresponding

to the thickness of one layer plus the interlayer space filled with organic surfactant. The thickness of the single layer is approximately 0.9 nm.

The surfactant solution is usually of a high pH and therefore the unintended side effect, a partial dissolution of the zeolitic material, can appear accompanied by creation of mesopore particles of M41S type[63]. To distinguish mesopore particles, a part of the swollen IPC-1SW was calcined. Its XRD pattern confirmed the burning of the surfactant and contraction of the interlayer space as the (200) reflection shifted to higher 2θ values, 10.1˚ (2θ) (**Fig. 9**). In the low angle area where reflections for M41S particles are expected, no peaks were observed. The calcined IPC-1SW is very similar to calcined hydrolysed IPC-1P, designated as IPC-1, where (200) peak is also shifted to higher position at 9.9˚ (2θ). The shift of the (200) and low intensity of intralayer peaks in both calcined materials insinuate the contraction of the interlayer space and not well-ordered condensed layers (further discussed in **Chapter 4.1.2**).

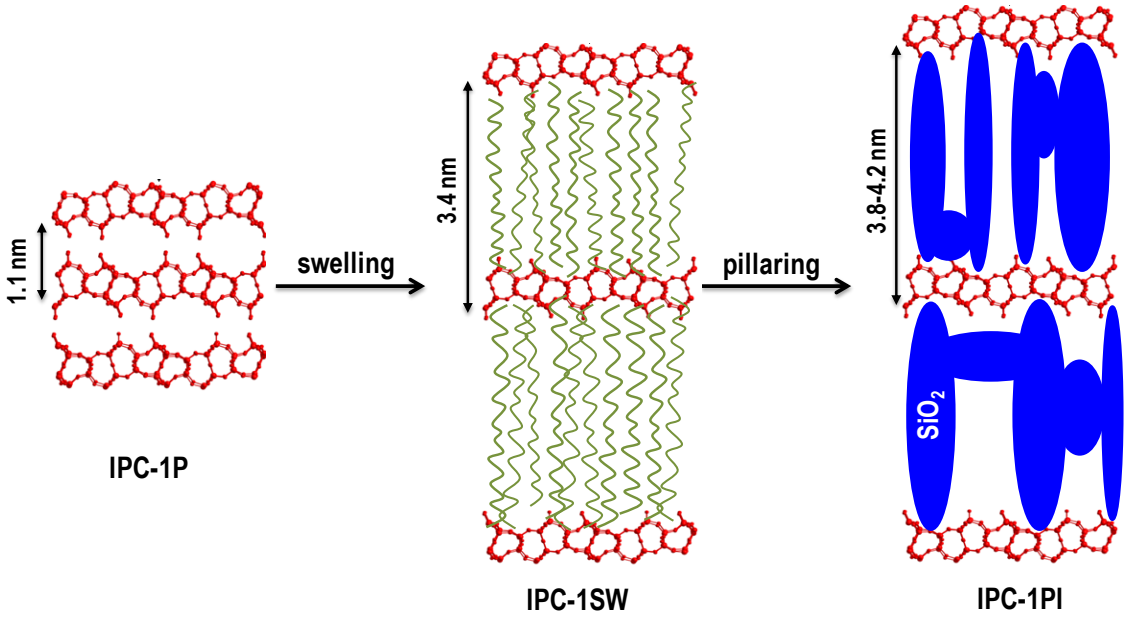

Scheme 2 The schematic view on the layer manipulation using long organic surfactant (C_{16}TMA in green) for swelling and subsequently tetraethyl orthosilicate (TEOS) for creation of amorphous silica pillars between the layers (the blue colour represents the amorphous silica between the layers).

The following pillaring treatment of IPC-1SW stabilizes the structure in the meaning of preserving the increased interlayer distance even after calcination. It was achieved by adding of silica source in the form of tetraethyl orthosilicate. After calcination the interlayer space is partially filled with amorphous silica in the form called pillars. The nature and arrangement of the silica pillars are unknown and hard to determine. Based on the weight balance it is supposed that pillared IPC-1PI materials comprise of 30-50 wt.% of amorphous silica. The interlayer space expansion is confirmed by the XRD pattern where the (200) reflection was shifted to 2.2˚ (2θ) corresponding to 4.1 nm. The peak is slightly broader insinuating the wider range of interlayer spacing.

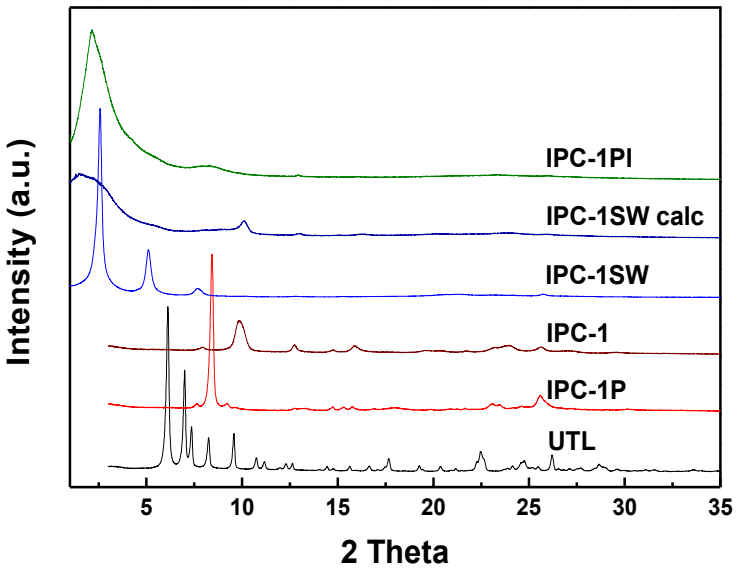

Fig. 9 XRD pattern of parent UTL zeolite in comparison to hydrolysed IPC-1P, calcined hydrolysed IPC-1, swollen IPC-1SW, its calcined form IPC-1SW calc, and pillared IPC-1PI (calcined).

All structural changes during the post-synthesis modifications were reflected in the textural properties of IPC-1 materials, which were evaluated by analysing argon adsorption isotherms. The argon isotherms of parent UTL and its post-synthetic modified forms are displayed in **Fig. 10** and the values of specific surface area and pore volumes are given in **Table 1**. Parent zeolite UTL has the adsorption-desorption isotherm of type I according to IUPAC classification[64]. Its isotherm shows a steep increase in the adsorbed amount in the region of low relative pressures ($p/p_0 < 0.01$) as the micropores are filling. The long horizontal plateau at $p/p_0 > 0.01$ is typical for microporous material. The specific surface area BET is equal to 500 m^2/g and the micropore volume is 0.290 cm^3/g. Its pore size distribution is centred at 0.65 nm corresponding to 14-12-ring channel system of UTL.

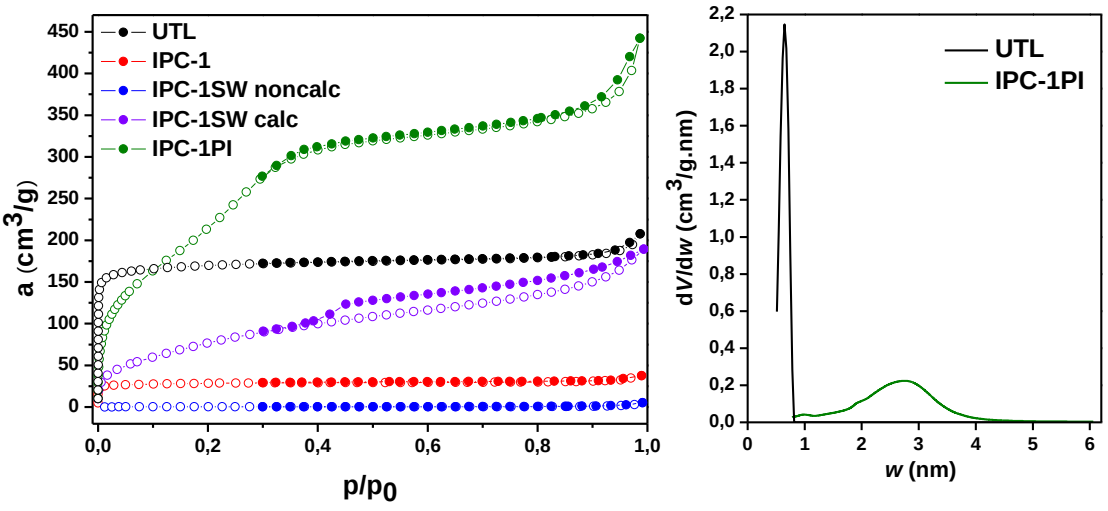

Fig. 10 Adsorption-desorption isotherms of argon measured at -186 °C (left) and the pore size distribution measured on argon (right). The solid points denote desorption branch.

Table 1 The position of the interlayer (200) peak and corresponding d-spacing values for parent UTL and all modified IPC-1 materials including textural data from argon adsorption measured at -186 °C.

Material	XRD		Argon sorption data		
	(200) peak (° 2θ)	d-spacing (nm)	BET (m^2/g)	V_{tot} (cm^3/g)	V_{mic} (cm^3/g)
UTL	6.15	1.44	500	0.301	0.290
IPC-1P	8.43	1.05	-	-	-
IPC-1 calc	9.90	0.90	92	0.059	0.043
IPC-1SW noncalc	2.58	3.42	2	0.008	-
IPC-SW calc	10.08	0.88	257	0.233	0.035
IPC-1PI	2.16	4.09	777	0.537	0.082

The layered IPC-1P was calcined before sorption measurement to remove the water adsorbed between the layers. The contraction of the interlayer space observed in the XRD pattern (**Fig. 9**) was confirmed by the sorption measurement when the BET area in IPC-1 decreased to 92 m^2/g. Since the D4R units between the layers were removed, there is no channel system coming through the solid layers, thereby the total and micropore volumes significantly decreased to 0.059 and 0.043 cm^3/g, respectively. After swelling of IPC-1P, the non-calcined IPC-1SW did not adsorb almost any argon (BET = 2 m^2/g) as the interlayer space is stuffed with the molecules of long-chain surfactant. The layers themselves do not possess any porosity hence, the total pore volume is negligible (V_{total} = 0.008 cm^3/g). However, the calcination of the sample and burning out the organics caused the layer condensation. As the result the argon isotherm shows gradual increase in the adsorbed amount and a hysteresis loop in the desorption branch. It will be discussed further that UTL and all IPC-1 materials have the same morphology of very think rectangular crystals. The stacking of the hydrolysed layers is aligned along the *a* axis, along the shortest dimension of the crystal. Therefore, some delamination or aggregation of the layers can be expected after calcination of IPC-1SW. In its isotherm, the continuous uptake of the adsorbed amount is caused by filling of the interparticle space and hence BET surface area increased to 257 m^2/g as well as the total pore volume, 0.233 cm^3/g. According to XRD pattern (**Fig. 9**), the calcined IPC-1SW and calcined IPC-1 reveal the similar character. However, their origin is distinct and the more disordered structure of calcined IPC-1SW is reflected in the different shape of adsorption isotherm and the different BET area and total pore volume.

After pillaring of IPC-1SW, the final IPC-1PI shows absolutely distinct profile of adsorption-desorption isotherms from the other members of IPC-1 family. The isotherm gradually increases in the region p/p_0 0.01-0.3, which is typical for mesoporous materials with mesopores below 4 nm[65]. The BET area is the highest from IPC-1 family, BET = 777

m^2/g, and its mesopore character is reflected in the higher total pore volume, which increased up to 0.537 cm^3/g (**Table 1**). The pore size distribution displayed in **Fig. 10** is centred at 2.7 nm. It is clear from broader range of mesopore sizes that the mesopores, created by introduction of amorphous silica, are not uniform in size or shape. The value 2.7 nm roughly corresponds to the data determined from XRD pattern, where d-spacing was found 4.1 nm but this value includes the thickness of the layer (around 0.9 nm).

Generally, in most of pillared materials (including heterogeneously substituted with boron, iron or aluminium) the low angle peak appears in the range 2.1-2.3˚ (2θ) corresponding to 3.8-4.2 nm. Consequently, their textural properties can slightly vary, e.g. the BET values are in the range 800-1100 m^2/g and the total pore volume 0.5-0.8 cm^3/g, however, the shape of isotherms follows the same trend. The examples of nitrogen isotherms of pillared materials prepared from pure germanosilicate UTL and heterosubstituted UTL zeolites are shown in **Fig. 11** with corresponding data in **Table 2**.

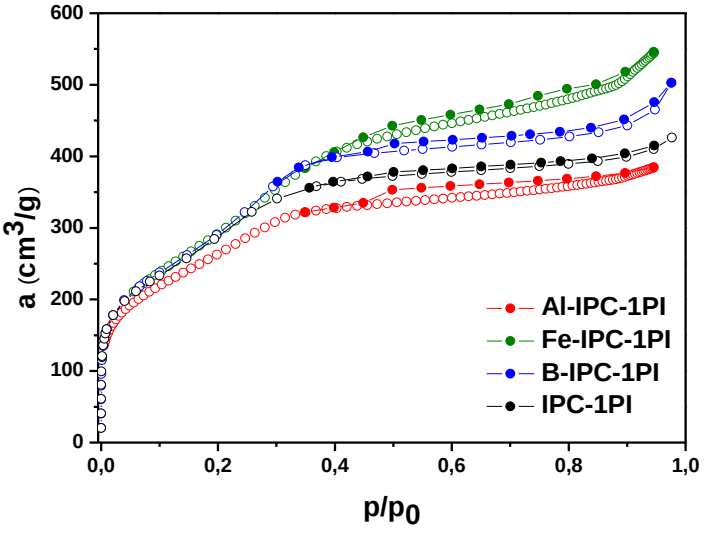

Fig. 11 Nitrogen adsorption isotherm measured at -196 °C of pillared.

Table 2 The position of the interlayer (200) peak and corresponding d-spacing values for pillared materials prepared from pure germanosilicate UTL and heterosubstituted UTL zeolites including textural data from nitrogen adsorption measured at -196 °C.

Material	XRD		Nitrogen sorption data		
	(200) peak (˚ 2θ)	d-spacing (nm)	BET (m^2/g)	V_{tot} (cm^3/g)	V_{mic} (cm^3/g)
IPC-1PI	2.16	4.09	1085	0.534	0.014
B-IPC-1PI	2.19	4.03	1090	0.785	0
Fe-IPC-1PI	2.21	3.99	1119	0.843	0
Al-IPC-1PI	2.21	3.99	970	0.594	0

Scanning and transmission electron microscopy were used to study the integrity of UTL zeolite and its layers during the treatments and to confirm changing of spacing values. Zeolite UTL crystallizes in the form of rectangular crystals of an average size about 10 x 10 μm. The microplates are so thin (approximately 0.01-0.1 μm) they can be even bent like it is shown in **Fig. 12 (a)**. The hydrolysis of UTL leading to layered IPC-1P does not affect the particles morphology (**Fig. 12 (b)**). However, after the swelling the plate crystals are thicker (**Fig. 12 (c)**) in comparison to IPC-1P. As mentioned above, the layers in IPC-1P are stacked along the shortest dimensions of the crystals. Therefore, the thicker crystals in IPC-1SW are consistent with the model of the interlayer space expansion by adding of the long-chain organic surfactant. In the pillared IPC-1PI the microplates are more broken and damaged and they tend to aggregate. It is caused by severe conditions used during the swelling (high pH) and pillaring treatment.

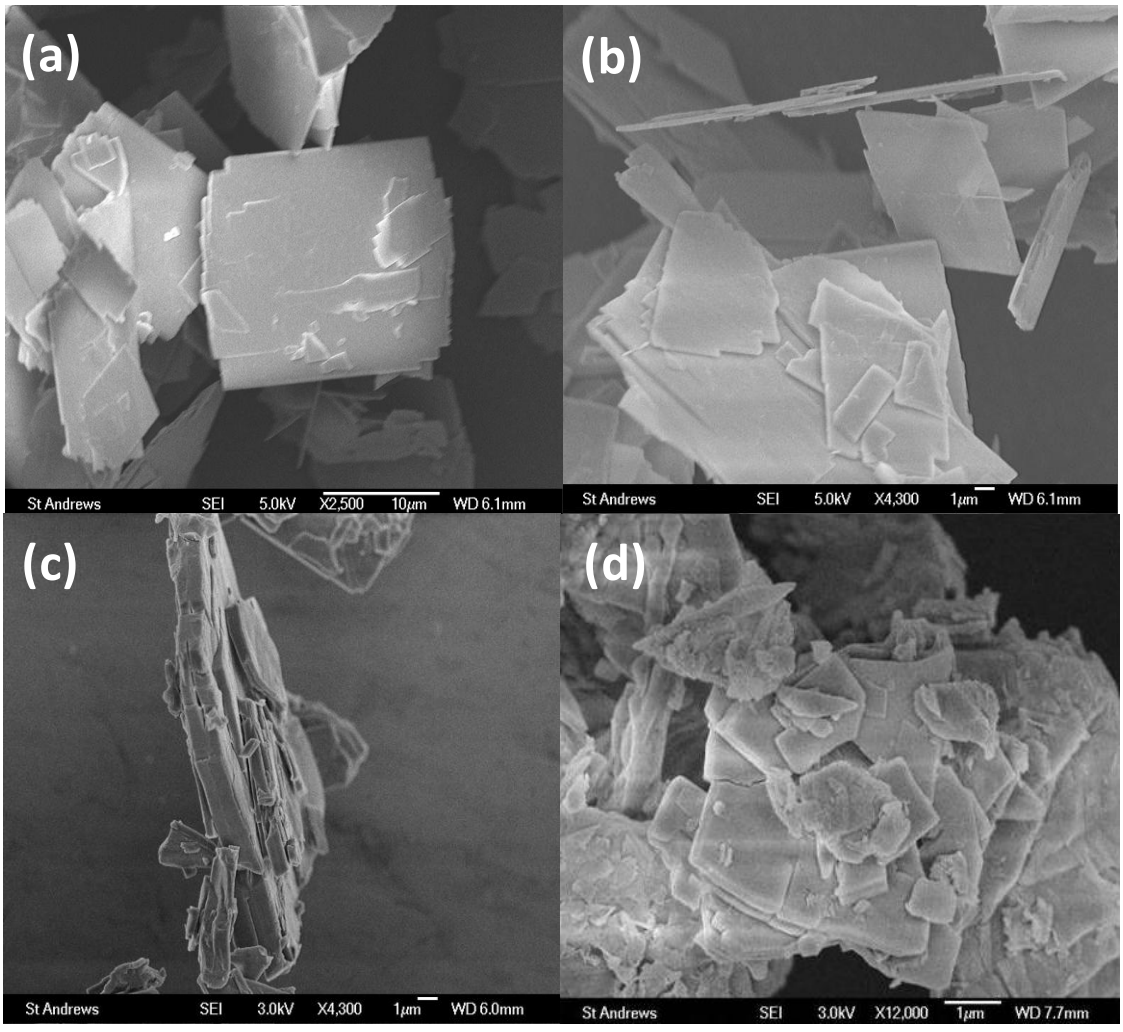

Fig. 12 SEM images of parent UTL **(a)**, hydrolysed IPC-1P **(b)**, swollen IPC-1SW **(c)** and pillared IPC-1PI **(d)**.

The microstructures of the materials were investigated by high resolution transmission electron microscope (HRTEM). The images of both hydrolysed calcined IPC-1 and pillared IPC-1PI materials demonstrate the layered character along the *b* axis (**Fig. 13**). The interlayer spacing for IPC-1 measured at 0.9 nm is in excellent agreement with the d-spacing from XRD pattern, 0.9 nm. The value corresponds to poorly condensed layers. In the pillared material, IPC-1PI, there is a clear increase in the interlayer spacing up to 3.7 nm, with a slight variation (±0.1 nm) depending on the crystallite measured. It is consistent with the d-spacing measured from XRD, where the peak has the maximum corresponding to 4.1 nm, but it is slightly broader indicating a wider range of interlayer spacing. **Fig. 13 (c)** highlights some very thin plates showing a region of only one or two unit cell

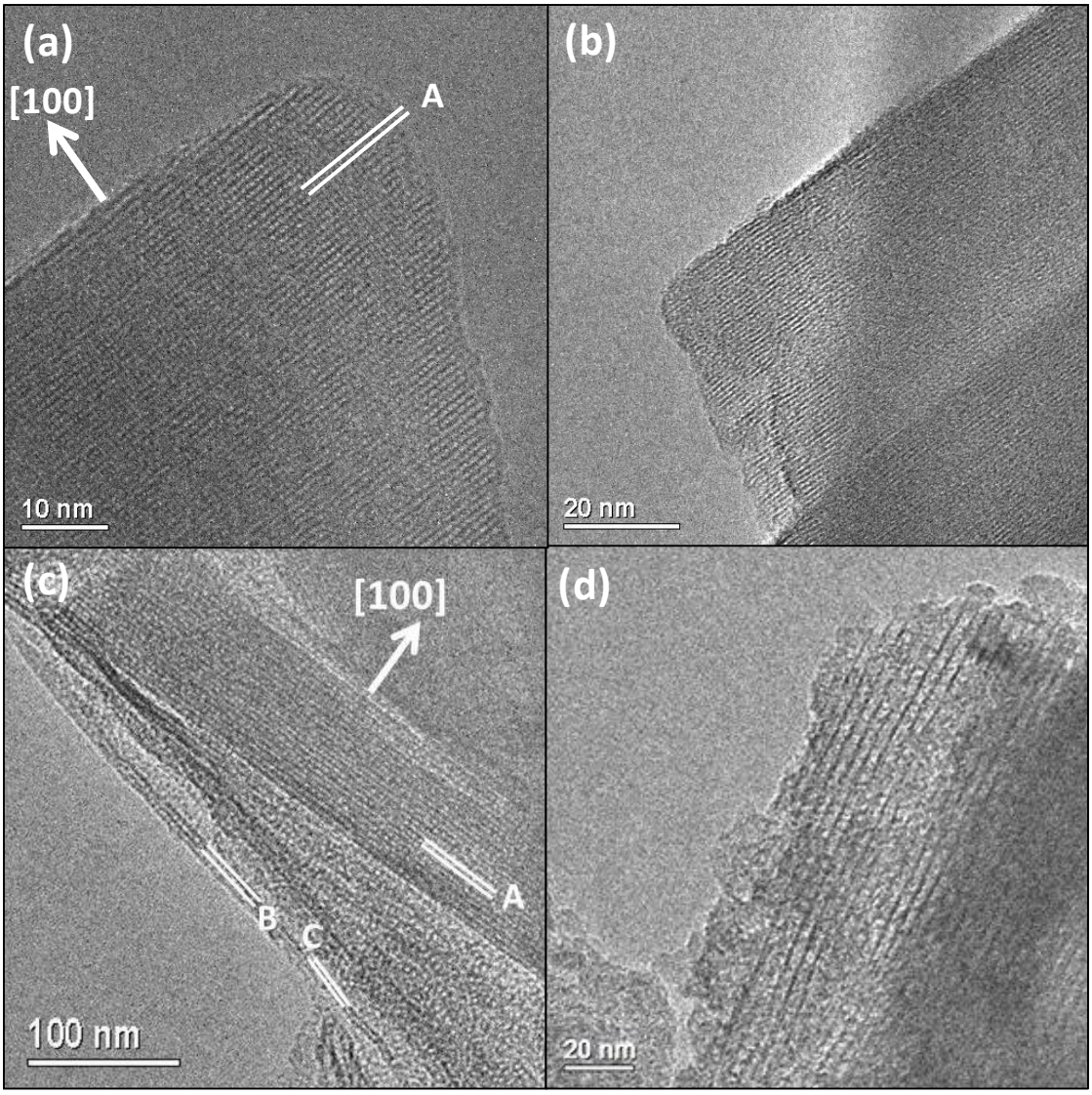

Fig. 13 High resolution TEM images: **(a,b)** hydrolysed calcined IPC-1 viewed down the [001] zone axis, showing the d-spacing of (A) 0.9 nm indexing to (200). **(c,d)** pillared IPC-1PI, showing the typical d-spacing of (A) 3.7 nm. Some very thin plates are also marked with thicknesses of 2 unit cells (B), 7.5 nm and 1 unit cell (C), 3.7 nm.

thickness. Such plates were likely exfoliated from the thicker particles. Overall, HRTEM images indicate that the UTL layers remain intact during all the treatments. The electron diffraction measured on IPC-1 family confirmed the integrity of the layers and their UTL character, which stay untouched during all post-synthesis modifications.

To summarize the results, the lamellar character of IPC-1P offers the opportunity of manipulation with the layers similar as it was first demonstrated on MCM-22P[37]. The increasing of the interlayer space by intercalation of long-organic chain surfactant and amorphous silica led to a new pillared material. IPC-1PI preserves the UTL character of the layers, which are delayed from their original positions about 3 nm. Unlike pillared MCM-36[39] prepared from MCM-22P, IPC-1PI does not possess any micropores and hence any shape-selectivity in catalytic reactions cannot be expected (discussion in **Chapter 4.3**). Still, the ultrathin zeolite layers and the modification of the interlayer distance can increase the accessibility to important reactive sites located mainly on the layer surface.

4.1.2 New three-dimensional zeolites IPC-2 and IPC-4

The swelling and pillaring treatments showed how the rigid layers of IPC-1P can be manipulated and the interlayer distance and space can be modified. In attempt to connect the layers back to form new three-dimensional structure, IPC-1P was silylated with diethoxydimethylsilane. The procedure known for other layered zeolites as stabilization[42] led in the case of IPC-1P to new three-dimensional zeolite. After hydrolysis there are a lot of silanol groups on the layer surface[66]. The terminal silanols from removed D4R units react with ethoxy groups of the silane and thus, the silylating agent acts as the bridging molecule between the layers. The silanol groups are very close to each other and after calcination they condense into new single-four-rings (S4Rs). In the XRD pattern the (200) peak is shifted to lower (2θ) values, 7.7˚ (2θ) corresponding to higher d-spacing compared with IPC-1P (**Fig. 14**).

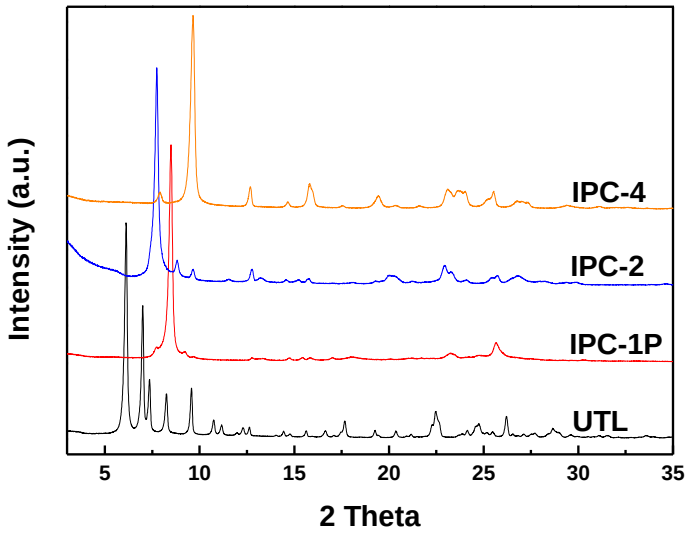

Fig. 14 XRD pattern of parent UTL, layered IPC-1P and new zeolites IPC-2 and IPC-4.

In contrast to other stabilized layered zeolites, e.g. IEZ-MWW, here the new silica bridges are interconnected in all three dimensions (in S4R), which is the fundamental premise of zeolite framework. The novel zeolite was denoted IPC-2. The replacement of the original D4R units by new S4Rs formed 12-10-ring channel system with relatively spherical windows of 0.66 x 0.62 and 0.53 x 0.52 nm (**Fig. 15**). For comparison the parent UTL zeolite has 14-12-ring channels with the opening pores 0.95 x 0.71 and 0.85 x 0.55 nm, respectively.

Recently, Verheyen and co-workers[67] prepared a material called COK-14, which is isostructural to IPC-2 zeolite. The material was prepared directly from UTL zeolite using 12M HCl solution. They denoted the mechanism as inverse sigma transformation[67]. COK-14 was verified as a new zeolite with the three-letter abbreviation **OKO**[7].

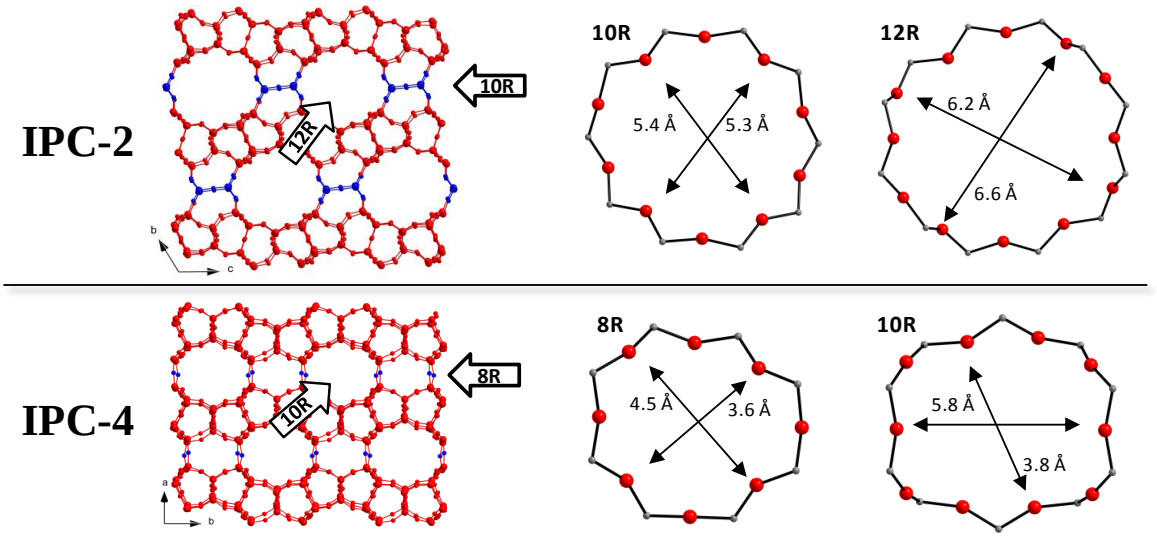

Fig. 15 The pore windows and sizes for zeolites IPC-2 and IPC-4.

Based on the knowledge that layers are possible to condense into new zeolite by adding the source of silica for building S4R units (IPC-2), it was assumed that the IPC-1P layers could condense directly without additional silica source. However, the direct calcination of IPC-1P led to the material with very low intensity of XRD diffraction lines (see IPC-1 in **Fig. 9**) and low BET surface area (92 m^2/g) as well as the micropore volume (0.043 cm^3/g) (**Fig. 10**, **Table 1**). This material denoted as IPC-1 is composed of not-well condensed layers. Therefore, the IPC-1P was first intercalated with various types of amines or ammonium salts (e.g. octylamine or tetrapropylammonium cation) helping to organise the layers. After calcination the XRD pattern shows the shift of (200) peak to 9.7˚ (2θ) similar as in IPC-1, nevertheless all diffraction lines are more intensive (**Fig. 14**). The new material was designated IPC-4. The intercalation of organic molecules between the layers facilitates the organisation of the layers in the most suitable position and during the calcination surface SiOH groups on the up-and-down layers condensed. It was found that higher calcination temperature (up to 750˚ C) supports the full condensation of the silanol

groups (confirmed by ^{29}Si MAS NMR). The replacement of D4Rs in UTL by single Si-O-Si interlayer links is reflected in the size of the new channel system – 10-8-ring channels with openings of 0.58 x 0.38 nm for 10-ring and 0.45 x 0.36 nm for 8-ring (**Fig. 15**). The 10-ring is of ellipsoidal shape, which may be beneficial for selective isomerization of small hydrocarbons. Zeolite IPC-4 was verified by IZA Structure Commission as the novel zeolite with the three-letter code **PCR** (**P**rague **C**hemistry fou**R**)[7].

The new approach used for the synthesis of two new zeolites from one parent material was called **ADoR** strategy. The abbreviation means first it is necessary to synthesize the parent zeolite - **A**ssembly, then hydrolyse it into layered material – **D**isassembly, followed by **o**rganisation of the layers and finally calcination into new material – **R**eassembly (**Scheme 3**). The organisation step before reassembly is not always necessary (*vide supra* IPC-1 vs. IPC-4) and thus, it is represented in the abbreviation by a small letter. Nevertheless, the intercalation of the organic groups helps the proper and full condensation of the surface silanol groups.

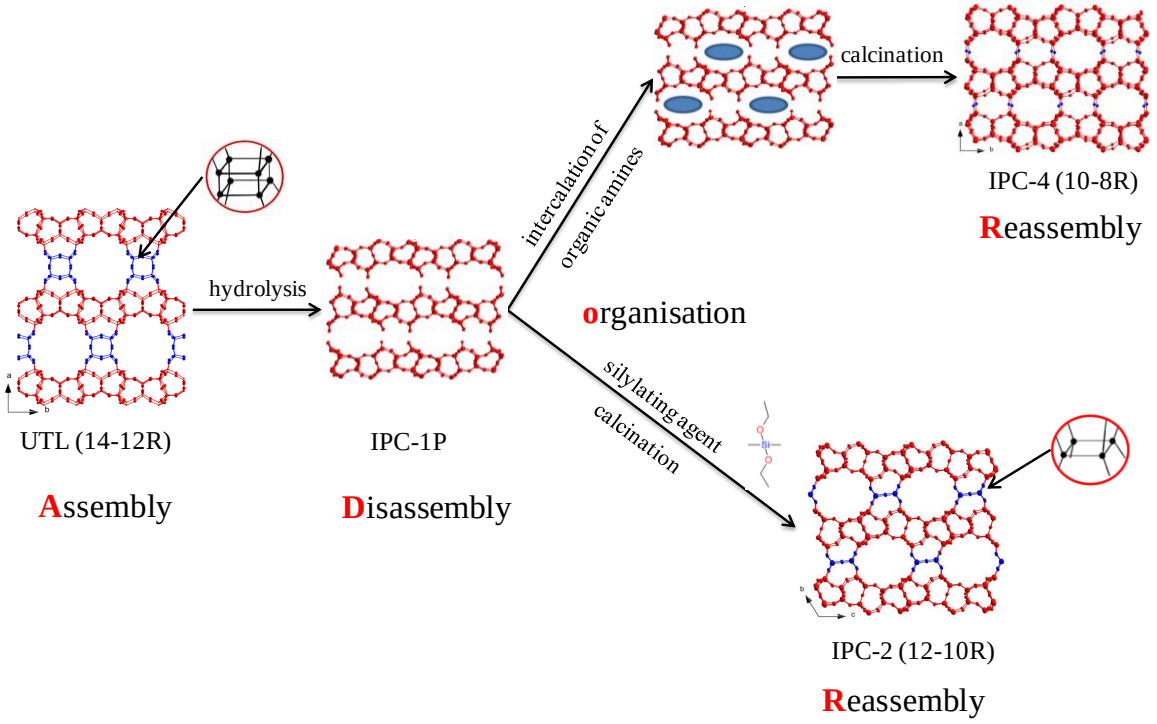

Scheme 3 The scheme for synthesis of new zeolites from UTL by the ADoR method.

The argon isotherms in **Fig. 16** demonstrate the differences in the arrangement of the layers in zeolites UTL, IPC-2 and IPC-4. The data are summarized in **Table 3**. All three zeolites are microporous and the micropore volumes decrease in the order UTL (0.290 cm^3/g) > IPC-2 (0.191 cm^3/g) > IPC-4 (0.115 cm^3/g) and reflects the changes in the pore dimensions 14-12-ring (UTL) > 12-10-ring (IPC-2) > 10-8-ring (IPC-4). The specific surface area decreases in the same order UTL (500 m^2/g) > IPC-2 (346 m^2/g) > IPC-4 (278

m^2/g). The pore size distribution in UTL is centred at 0.65 nm, in IPC-2 at 0.57 nm, but in IPC-4 the maximum is shifted to very low pore dimensions and cannot be reached by argon nor nitrogen adsorption.

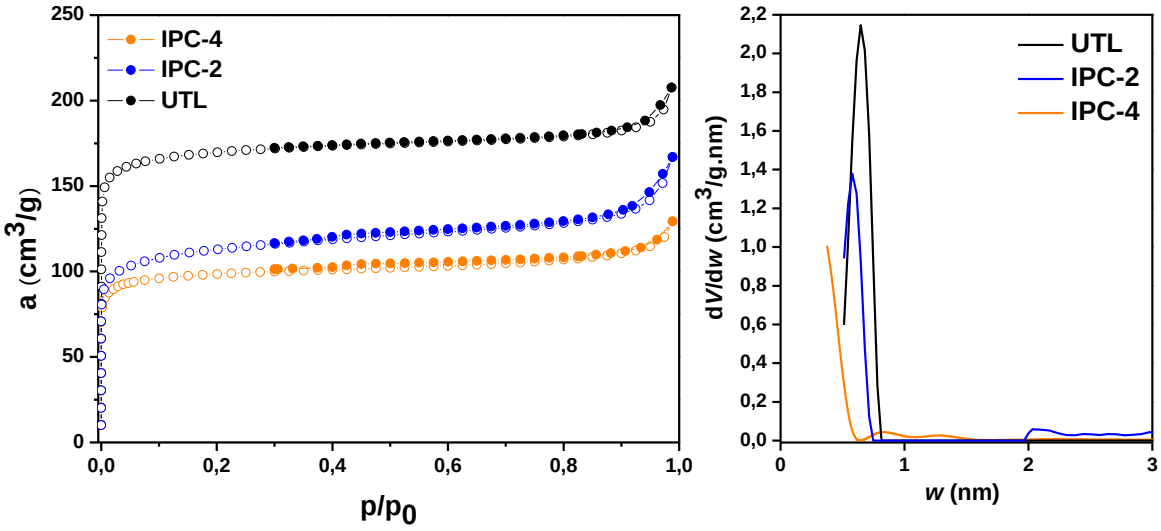

Fig. 16 Adsorption isotherms of argon measured at -186 °C (left) and the pore size distribution measured on argon (right). The solid points denote desorption branch.

Table 3 The position of the interlayer (200) peak and corresponding d-spacing values for parent UTL and new zeolites prepared by the ADoR method including textural data from argon sorption measured at -186 °C.

Material	XRD		Argon sorption data		
	(200) peak (° 2θ)	d-spacing (nm)	BET (m^2/g)	V_{tot} (cm^3/g)	V_{mic} (cm^3/g)
UTL	6.15	1.44	500	0.301	0.290
IPC-2	7.74	1.14	346	0.238	0.191
IPC-4	9.66	0.92	278	0.145	0.115

To summarize the results, two novel zeolites, IPC-2 (OKO) and IPC-4 (PCR), were prepared from a one parent UTL zeolite by a new approach called the ADoR strategy. In the first step, the UTL structure is unzipped/disassembled into layers, which can be further manipulated or even more important can be condensed/reassembled back. Choosing different linkers between the layers enables the synthesis of zeolites with predictable structure, namely the pore architectures.

4.2 The mechanism of the ADoR process

To study the mechanism of the ADoR process, especially the disassembly step, series of experiments using different concentrations of hydrochloric acid were performed. The same parent UTL zeolite with Si/Ge molar ratio 4.4 was hydrolysed in water, 0.1M, 6M and 12M HCl solution. The hydrolysis was stopped at various times (after 5 minutes, 1, 2, 8, 16 and 24 hours). With exception of the first 5 minutes when the experiment was done at room temperature, the reaction mixtures were heated up to 85 ˚C. The products were analysed by XRD powder diffraction and the chemical analysis was determined by Energy-dispersive X-ray spectroscopy (EDX). The liquid after hydrolysis was dried under vacuum to get a powder, which was as well analysed by EDX.

The experiments proved that the hydrolysis is an unusually fast process. After the first five minutes of UTL hydrolysis in various solutions, the recovered solids show almost identical XRD patterns (**Fig. 17A**). However, in time the differences are more considerable and the most noticeable between the neutral environment of water or slightly acid 0.1M HCl and highly concentrated acid solutions (**Fig. 17B**). **Fig. 18** compares the parent UTL and the solids after hydrolysis in 0.1M HCl in different time. Within 5 minutes there is no evidence for any remaining unhydrolysed UTL zeolite. Such rapid process is explained by the excellent accessibility to germanium-D4R units via the pores of UTL. After 5 minutes the position of the dominant peak (200) is shifted to higher angle values but is also broader (**Table 4**). The full width at half-maximum (FWHM) for interlayer peak (200) in parent UTL is 0.124˚ (2θ) while after 5 minutes in 0.1M HCl it increased to 0.388˚ (2θ) indicating the significantly shorter coherence length in the direction perpendicular to the layers. It means that the stacking of the layers is not very regular. However, in time the peak

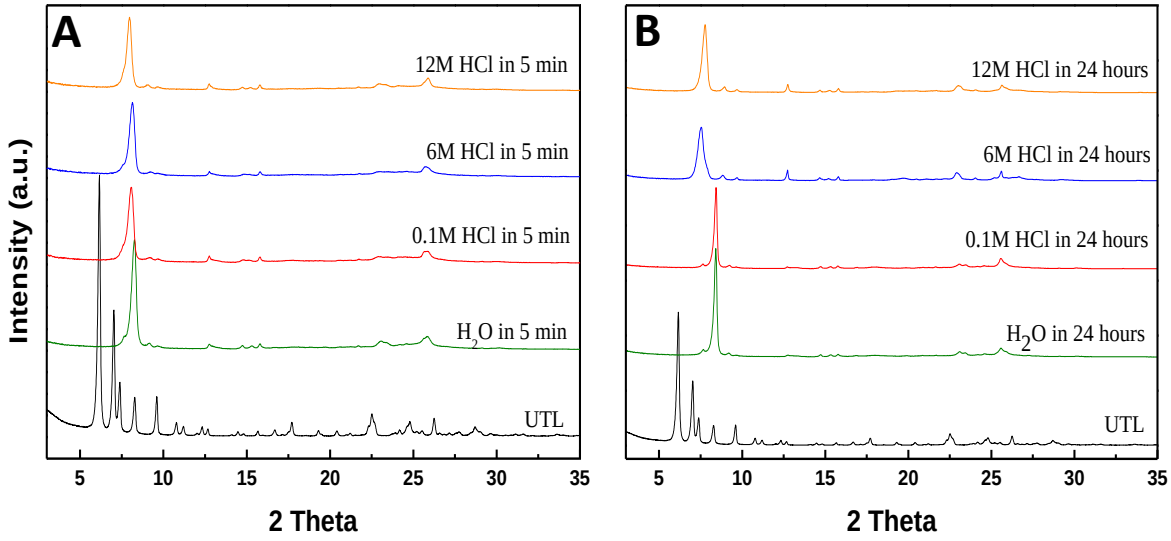

Fig. 17 XRD patterns of parent UTL zeolite and the solids hydrolysed in different solutions after 5 minutes at ambient temperature (**A**) and after 24 hours at 85˚ C (**B**). The materials are as-synthesized, not calcined.

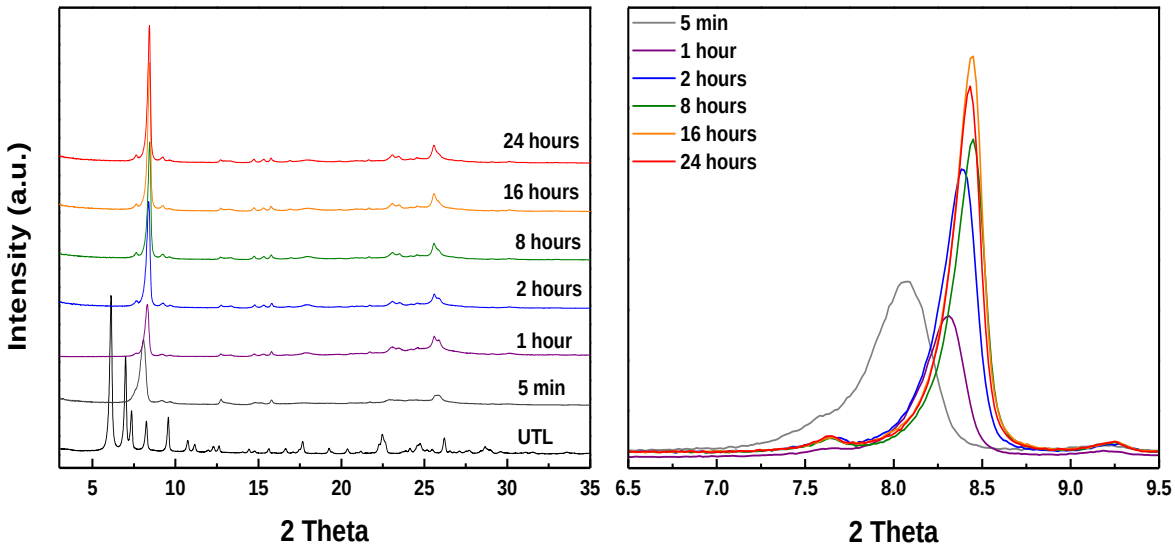

Fig. 18 XRD pattern of parent UTL and its hydrolysed forms using 0.1M HCl at 85 ˚C in different time (left). The interlayer (200) positions in different hydrolysis time (right).

becomes sharper and after 24 hours it is almost as narrow as in the parent UTL, FWHM 0.162˚ (2θ) and 0.124˚ (2θ), respectively. With the peak narrowing the (200) gradually shifts to higher angles indicating a continual, steady contraction of the interlayer space (from 1.44 nm in parent UTL to 1.05 nm after 24 hours of hydrolysis in 0.1M HCl).

The composition of the hydrolysed material in each step as well as the composition of the solution after hydrolysis is included in **Table 4**. Already after 5 minutes the Si/Ge ratio increased from original 4.4 in UTL up to 26 evidencing that most of Ge from D4Rs was removed and is present in the solution (Si/Ge ratio 5.3). In time the Si/Ge ratio in the solid was increasing and after 24 hours it reached 89 evidencing pure silica layers with the minimum amount of germanium in them.

Table 4 The position of the interlayer peak (200), its corresponding d-spacing value and the value of full width at half-maximum (FWHM) for parent UTL zeolite and its hydrolysed forms in different time using 0.1M HCl. The chemical analysis of hydrolysed solids and powders from dried solutions after hydrolysis was determined by EDX.

Hydrolysis time	(200) peak (˚ 2θ)	d-spacing (nm)	FWHM (˚ 2θ)	Si/Ge in solid	Si/Ge in solution
0 (parent UTL)	6.15	1.44	0.124	4.4	-
5 minutes	8.07	1.10	0.388	25.8	5.3
1 hour	8.31	1.07	0.265	46.0	4.2
2 hours	8.40	1.05	0.204	65.0	3.5
8 hours	8.45	1.05	0.184	79.0	2.4
16 hours	8.45	1.05	0.163	71.9	1.6
24 hours	8.44	1.05	0.162	88.9	2.6

Overall, the process of hydrolysis in neutral or slightly acid solution is very rapid as well as removing of species (atoms) from the interlayer space resulting in the interlayer contraction. Hence, the process was denoted as *de-intercalation*. The UTL-like layers remain without any residue from D4R or S4R units. The direct calcination of the material (IPC-1P) led to the formation of IPC-1/IPC-4 by condensation of the surface silanol groups. However, as it was discussed above (**Chapter 4.1.2**), without previous organisation of the layers (by intercalation of organic molecules) the layers are not fully condensed and/or are less ordered (*vide supra* IPC-1 vs. IPC-4).

On the other hand, using the 12M HCl solution shows the opposite trend in the behaviour (**Fig. 19**, **Table 5**). In the first two hours a small shift to the higher angles was observed as well as a broad band between 10-20˚ (2θ) attributed to partial amorphization. Nevertheless, after next couple of hours the crystallinity returned, but the (200) moved to lower angles and after 24 hours finishes at 7.76˚ (2θ). Such behaviour corresponds to the fast hydrolysis of the D4R units, but unlike 0.1M HCl hydrolysis, the species remain between the layers. In time they rearranged into the material similar to IPC-2, so called IPC-2-precursor. The EDX analysis proved the removing of Ge and the presence of Si in solutions in first few hours. It is the consequence of partial amorphization, although, over time the Si/Ge ratio in solutions was decreasing as atoms were incorporated back into the framework (**Table 5**). The process was designated as *rearrangement* and leads to a new structure where new silica single-four-ring (S4R) units are attached to each of the UTL-like layers. The calcination of the IPC-2-precursor formed IPC-2 structure.

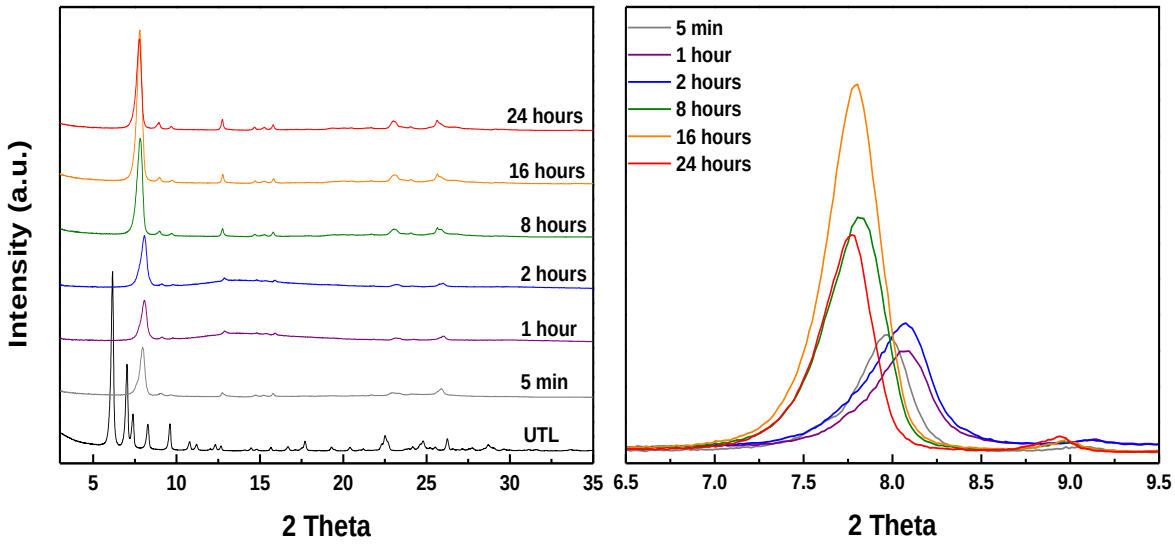

Fig. 19 XRD pattern of parent UTL zeolite and hydrolysed forms using 12M HCl at 85 ˚C in different time (left). The interlayer (200) positions in different hydrolysis time (right).

Table 5 The position of the interlayer peak (200), its corresponding d-spacing value and the value of full width at half-maximum (FWHM) for parent UTL zeolite and its hydrolysed forms in different time using 12M HCl. The chemical analysis of hydrolysed solids and powders from dried solutions after hydrolysis was determined by EDX.

Hydrolysis time	(200) peak (˚ 2θ)	d-spacing (nm)	FWHM (˚ 2θ)	Si/Ge in solids	Si/Ge in solution
0 (parent UTL)	6.15	1.44	0.124	4.4	-
5 minutes	7.97	1.11	0.306	33.0	1453.8
1 hour	8.06	1.10	0.306	78.6	108.6
2 hours	8.06	1.10	0.326	86.3	103.0
8 hours	7.81	1.13	0.367	98.4	46.2
16 hours	7.78	1.14	0.326	49.0	28.6
24 hours	7.76	1.14	0.347	51.5	48.1

Overall, the first couple of minutes in hydrolysis does not depend on the conditions applied and have the same progress (removing of most germanium). Afterwards two processes of de-intercalation and rearrangement compete and the crucial factor is the H^+ concentration. The neutral or slightly acid conditions (water or 0.1M HCl) favour the removing of atoms between the layers – de-intercalation. Conversely, the highly concentrated HCl favours the rearrangement of the species between the layers. The end products are zeolites IPC-4 (in the case of de-intercalation) and IPC-2 (in the case of rearrangement) (**Scheme 4**).

In the study performed at St. Andrews University it was found that the gradual changing of the H^+ concentration leads to shifting of the equilibrium between the de-intercalation and rearrangement processes. In the certain point (specific HCl concentration, 1.5M) the rate of de-intercalation and rearrangement are balanced and half of the layers undergo the de-intercalation and the rest (in the same crystal) undergoes the rearrangement. Reassembly of such material leads to a new structure denoted IPC-6, which can be seen as a structural combination of IPC-2 and IPC-4 zeolites with two independent pore systems of 12-10-ring and 10-8-ring size (**Scheme 4**). Based on experiments, it can be assumed that changing the HCl concentration from 0–12M HCl leads to the formation of materials composed of IPC-4 and IPC-2 from 0 to 100 % of each.

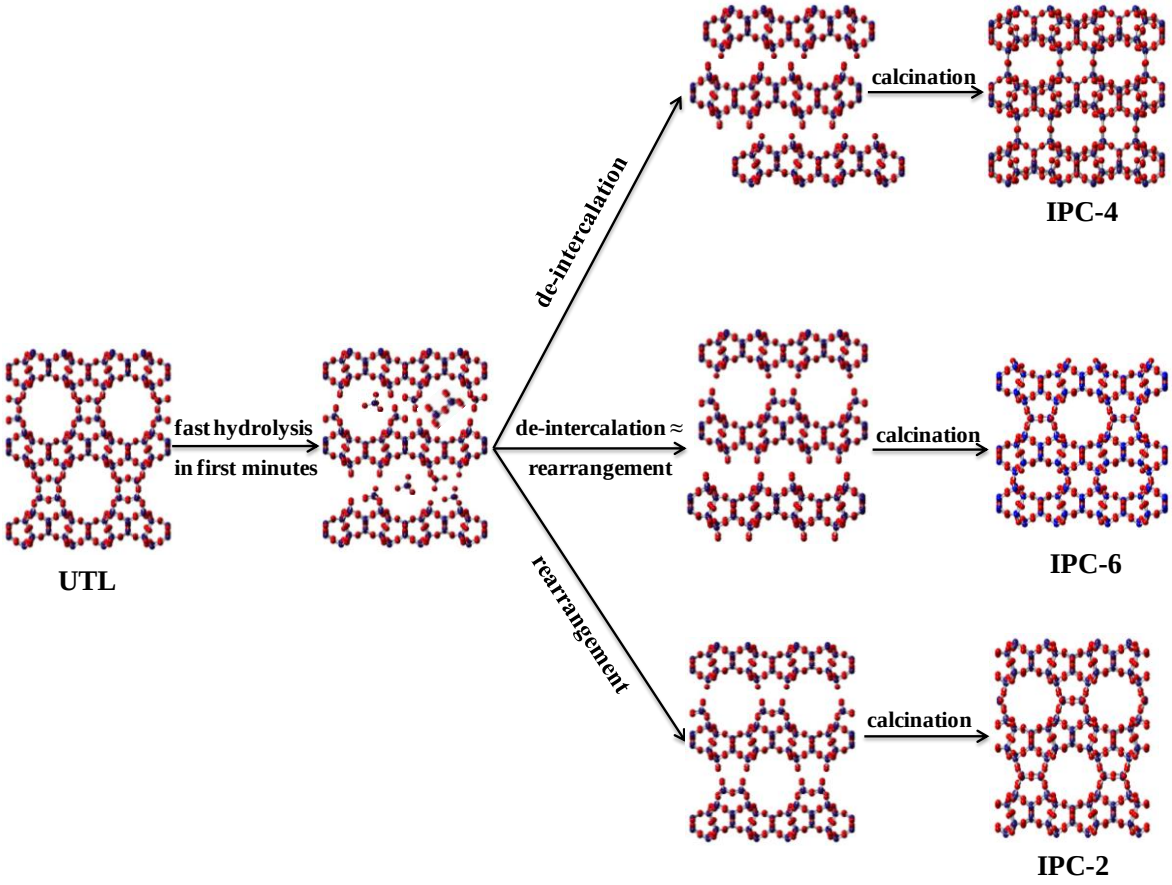

Scheme 4 The scheme of UTL disassembly depending on the solution acidity. The neutral or slightly acid environments enhance de-intercalation processes, while highly acid solutions favour rearrangement processes. Depending on the dominant process, the hydrolysis and subsequent calcination/reassembly of the material lead to the formation of zeolites IPC-2, IPC-4 or IPC-6.

4.3 Catalytic activity of new zeolites

4.3.1 Alkylation of toluene

Zeolites belong to the most important heterogenous catalysts in petrochemistry and in the synthesis of fine chemicals. In many processes they replaced catalysts like solid acids ($AlCl_3$, $FeCl_3$) and protonic acids (H_2SO_4, H_3PO_4), which represent serious environmental problems like corrosion of reactors, problems with separation, storage and harmful disposal.

The novel materials prepared from zeolite Al-UTL were tested for their catalytic activity in the transformation of aromatic hydrocarbons, which is one of the most important branches of petrochemistry. Alkylation of toluene with isopropyl alcohol was chosen as a model reaction to investigate the role of zeolite structure and acidic properties. The target product, *para*-cymene (**Fig. 20 1st step**), is a starting material for manufacturing pesticides, fungicides, flavours and heat media[68,69]. Nevertheless, *meta*-isomer is also important starting material for the production of intermediates and end products like cresols, fragrances, pharmaceuticals[68,69] etc. The most preferred isomer distribution requires low *ortho*-cymene content, since *ortho*-cymene is difficult to oxidize and inhibits the oxidation of the other isomers. The cymene isomers formed in the first alkylation step can subsequently react with toluene yielding undesired side products *n*-propyltoluenes (**Fig. 20 2nd step**).

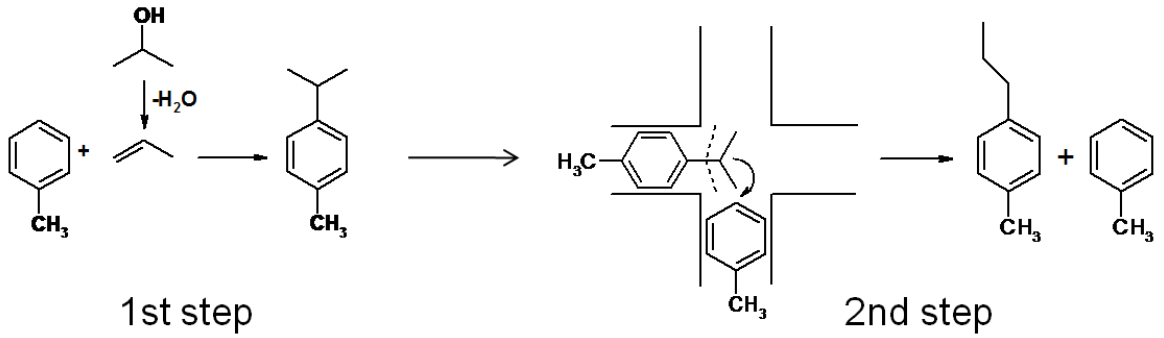

Fig. 20 The reaction scheme for alkylation of toluene with isopropyl alcohol (1st step) and the reactions leading to *n*-propyltoluenes (2nd step).

The catalytically active materials were prepared from Al-containing UTL by similar procedures described for pure germanosilicate UTL. The behaviour of novel materials, Al-IPC-1PI, Al-IPC-2 and Al-IPC-4, was compared with Al-UTL and standard zeolites MFI and BEA. Their structural characteristic and acidity determined by FTIR using acetonitrile as a probe molecule are summarized in **Table 6**.

Fig. 21 presents time-on-stream dependence of toluene conversions and some selectivities over zeolites under study. The molar ratio of toluene to isopropyl alcohol 9.6 was applied limiting the toluene conversion to about 10 % to exclude side reactions (e.g. toluene

disproportionation). The highest conversions of toluene were achieved using zeolites Al-BEA (8.8 % after 180 min of TOS) and Al-UTL (7.7 % after 180 min of TOS). Zeolites Al-MFI, Al-IPC-2 and Al-IPC-1PI were similarly active with conversions of toluene 5.1 %, 5.5 % and 4.5 % (after 180 min of TOS), respectively. The highest conversions of toluene were achieved over zeolites with the largest pore systems - 12-12-12-ring in Al-BEA (Si/Al = 23) and 14-12-ring in Al-UTL (Si/Al = 64), while over zeolites with smaller channel diameters like Al-MFI (10-10-10-ring, Si/Al = 35), Al-IPC-2 (12-10-ring, Si/Al = 70) or without any channels Al-IPC-1PI (Si/Al = 89) conversions of toluene were almost the same. In this perspective, the concentrations of Lewis and Brønsted acid sites seem to be of less importance than the dimensions of channel system and overall accessibility to active centres. Conversions of toluene were quite stable with TOS over all tested catalysts with exception of Al-IPC-2. The faster decrease in conversion of toluene, in the case of Al-IPC-2, can be explained by deactivation of catalyst by coking. Al-IPC-4 (Si/Al = 109) did not show practically any activity, which might be due to the presence of 10-ring channel, which is slightly ellipsoidal while the 8-ring one is too small to accept aromatic molecules. Nevertheless, the small size of channels and slightly ellipsoidal shape can be advantage in the isomerisation reactions of smaller hydrocarbons.

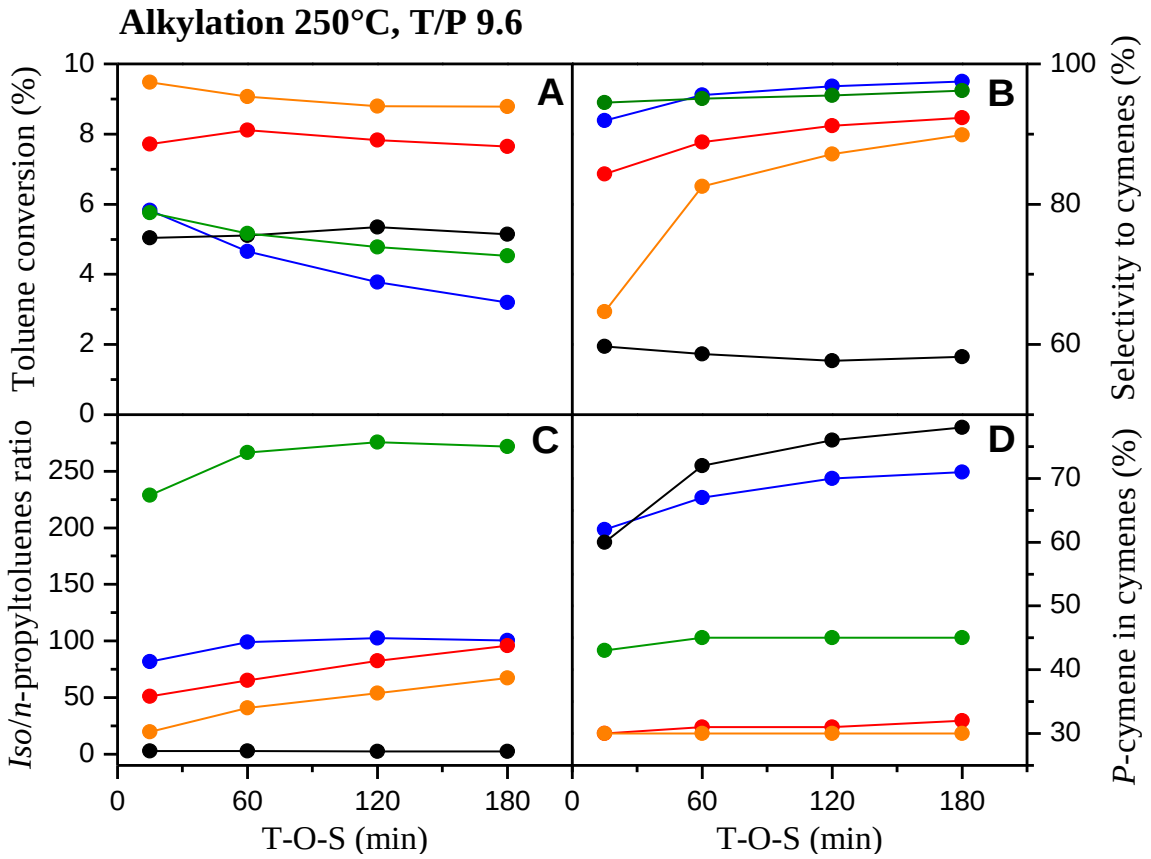

Fig. 21 Time-on-stream dependence of toluene conversion (A), selectivity to cymenes (B), *iso*-/*n*-propyltoluene ratio (C) and *para*-cymene selectivity (D) in toluene alkylation with isopropyl alcohol at 250 °C Al-MFI (●), Al-BEA (●), Al-UTL (●), Al-IPC-2 (●) and Al-IPC-1PI (●).

The selectivities to cymenes obtained over zeolites Al-MFI, Al-IPC-2 and Al-IPC-1PI were compared in 60 min of TOS at the conversion around 5 %. The selectivity to cymenes decreased in the sequence Al-IPC-2 (96 %) ≈ Al-IPC-1PI (95 %) > Al-MFI (59 %). The most frequent side products are *n*-propyltoluenes. The undesired products were formed over zeolite Al-MFI (*iso*/*n*-propyltoluenes ratio 2.5 after 60 min of TOS), while the pillared Al-IPC-1PI gave just its traces (*iso*/*n*-propyltoluenes ratio 267 after 60 min of TOS). As the pillared material does not possess any micropores inside the layers and the active centres are located only on the open layer surface, it can be supposed that Al-IPC-1PI acts similar to solid acids (like $AlCl_3$) where only *iso*-propyltoluenes are formed[70]. The *para*-selectivity over pillared Al-IPC-1PI and Al-IPC-2 reached 45 and 67 % while the highest percentage of *para*-cymene in cymens, 72 %, was achieved over Al-MFI, which correlates with the data in literature[71].

Table 6 The structural[7] and acid properties of tested zeolites.

Material	**FTIR (acetonitrile adsorption)**					**Channel system**	**Pore size (nm)**
	c_L mmol/g	**c_B mmol/g**	**Si/Al**	**$\%_L$**	**$\%_B$**		
Al-BEA	0.190	0.330	23	37	63	12, 3D	0.66 x 0.67, 0.56 x 0.56
Al-MFI	0.110	0.287	32	28	72	10, 3D	0.51 x 0.55, 0.53 x 0.56
Al-UTL	0.109	0.037	64	75	25	14-12, 2D	0.71 x 0.95, 0.55 x 0.85
Al-IPC-1PI	0.089	0.008	89	92	8	-	-
Al-IPC-2	0.102	0.029	70	78	22	12-10, 2D	0.62 x 0.66, 0.54 x 0.53
Al-IPC-4	0.055	0.041	109	57	43	10-8, 2D	0.58 x 0.38, 0.45 x 0.36

4.3.2 Hydroarylation of styrene

Using commercial zeolites one often faces the problems with diffusion limitations since the largest pore diameter in commercially used zeolites is 0.74 nm (in FAU). The pillared Al-IPC-1PI with no channels but mesopore character can offer the way to overcome the diffusion problems. Thereby, Al-IPC-1PI was tested in the catalytic reaction of bulky molecules.

The introduction of C-C bonds to arenes is a direct method for the synthesis of various biologically active compounds and pharmaceuticals like haplopappin, phenprocoumone, and avrainvilleol[72,73,74]. One of the reactions is the hydroarylation of styrene with phenols resulting in products with diarylmethane motive. The hydroarylation of styrene with phenol/*tert*-butylphenol was chosen as a model reaction to study the catalytic behaviour of pillared material (**Fig. 22**). The results were compared with commercial Al-BEA (for catalyst characteristics see **Table 6**).

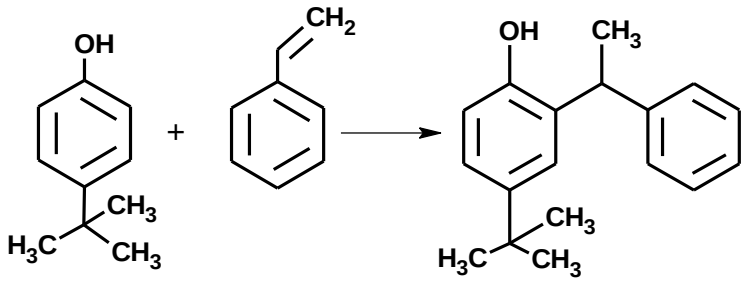

Fig. 22 The reaction scheme for styrene with *tert*-butylphenol.

In the reaction of styrene with phenol over zeolite Al-BEA almost 100 % conversion of styrene was achieved already in 20 minutes of the reaction time (**Fig. 23**). In the case of pillared Al-IPC-1PI, the 100 % conversion of styrene was achieved after 180 minutes. The selectivity to target product was in both cases 100 %. The faster increase in styrene conversion over Al-BEA can be attributed to its three-dimensional large channel system and higher concentration of Lewis and Brønsted acid sites (**Table 6**). Conversely, the pillared Al-IPC-1PI does not possess any micropores and the active centres are located only on the layer surface.

In the reaction of styrene with bulkier molecule of *tert*-butylphenol, the highest conversion of styrene achieved over zeolite Al-BEA was 81 % (in 300 min) while over pillared Al-IPC-1PI the conversion was 93 % (**Fig. 23**). The selectivity to target bulky product (**Fig. 22**) was 100 % over both materials. Despite Al-IPC-1PI possesses only low concentrations of acid sites (c_L = 0.089 mmol/g, c_B = 0.008 mmol/g), the pillaring treatment significantly enhanced the accessibility to them. Thereby, there should be no diffusion limitations often observed in commercial zeolites, like in zeolite Al-BEA. Nevertheless, without any channel system generally we cannot expect any shape-selectivity, which is one of the most important zeolite attributes utilized in catalysis.

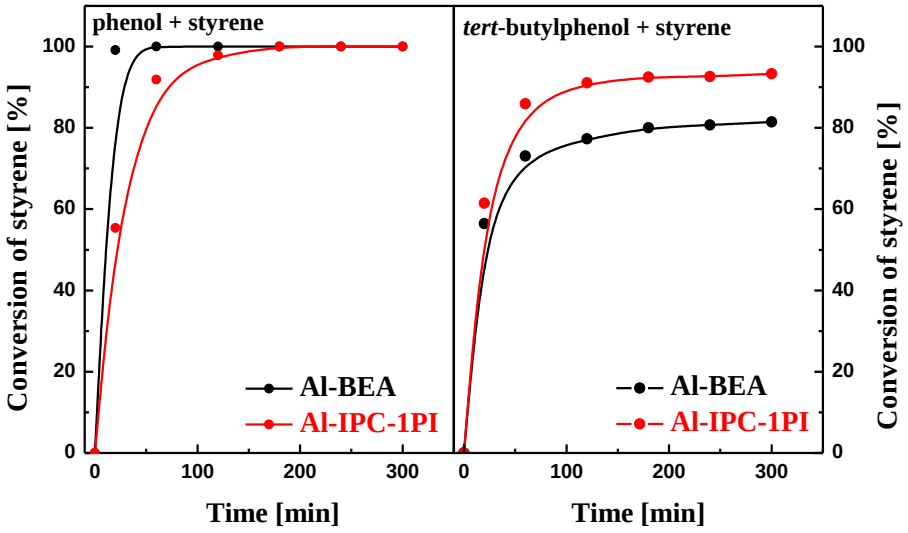

Fig. 23 The conversion of styrene in hydroarylation of styrene with phenol (left) and *tert*-butylphenol (right) over pillared Al-IPC-1PI and commercial Al-BEA zeolite.

Mentioning the mesopore character of Al-IPC-1PI (BET = 970 m^2/g, V_{total} = 0.594 cm^3/g), it should be noticed that a considerable part of the pillared material (usually 30–50 wt.%) is composed of amorphous inactive silica. **Fig. 24** compares the conversions of styrene in the reaction of styrene with phenol using different amount of catalyst. With less than 0.2 grams, pillared Al-IPC-1PI achieved higher conversion of styrene after 300 minutes in comparison with zeolite Al-BEA. Zeolite Al-BEA is necessary to use in the amount larger than 0.1 gram to reach better catalytic performance than pillared Al-IPC-1PI. It proves the unusually high accessibility to active centres presented mostly by Lewis acid sites.

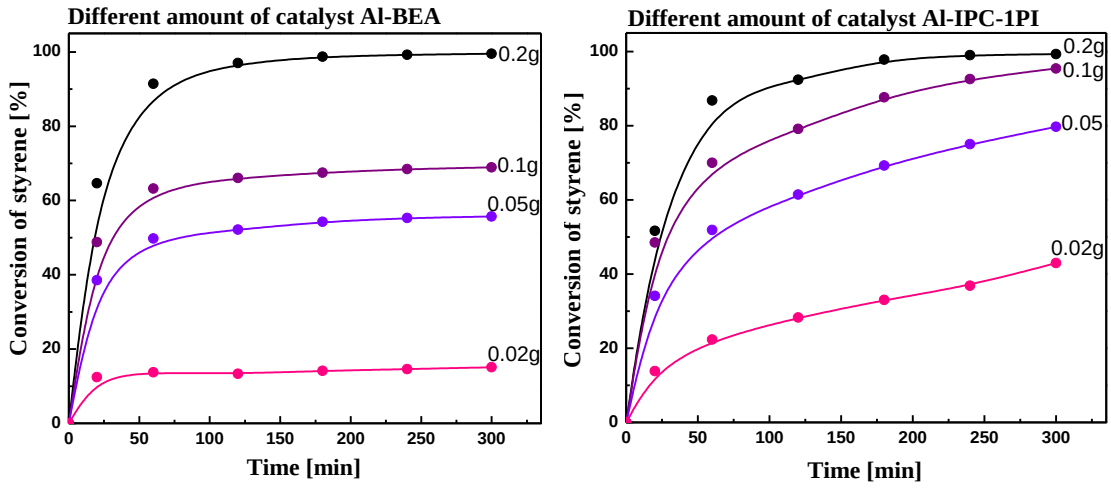

Fig. 24 The comparison of different amount of catalyst used in hydroarylation of styrene with phenol over zeolite Al-BEA (left) and pillared Al-IPC-1PI (right).

4.4 The general application of the ADoR strategy

The ADoR strategy provides a unique method to design and prepare new zeolitic structures through so called top-down synthesis. The great advantages are the preservation of the original zeolite character of the layers and the predictability of novel structures since it depends on the chosen linkage between the layers. The general application of the ADoR concept on other zeolites became the main target of the following research. Nevertheless, not each zeolite is suitable for testing. The crucial limits for choosing promising candidates are I) the presence of double-four-ring units, especially in the form of supportive building units between the layers, and II) the high content of germanium located mainly in D4Rs. Zeolites like IWR, ITH, ITR, and IWW belong to the suitable candidates. The application of the ADoR on IWW will be discussed in details in the next chapter.

4.4.1 Zeolite IWW and its 3D-2D-3D transformation

IWW was prepared as pure germanosilicate with two different compositions as Ge-rich IWW (Si/Ge molar ratio 3.1-3.6) and Ge-poor IWW (Si/Ge 6.4). Both materials were investigated by diffraction using synchrotron X-ray radiation and subsequent Rietveld refinement at the Laboratory of Crystallography in Zürich. It was found that the composition of D4R units in Ge-rich IWW is [6Ge,2Si] and in Ge-poor IWW [4Ge,4Si]. Hence, in Ge-rich IWW a complete almost purely germanium 4-ring can be expected to be dissolved during the acid treatment, as well as part of the other 4-ring composed by mixed T positions Si/Ge. In the case of Ge-poor IWW, all T sites in the D4R are of mixed Si/Ge positions. Theoretically, the acid treatment would lead only to an extraction of some atoms rather than complete disassembly of D4Rs and unzipping the structure into layers.
Based on the location of Ge in Ge-rich and Ge-poor IWW, Ge-rich IWW was predisposed to be easily hydrolysed into layered material, thereby the hydrolysis was tested under different conditions (see **Table 7**) and will be discussed first.

Table 7 Examples of conditions used for hydrolysis of Ge-rich IWW (Si/Ge ratio 3.1-3.6).

Sample	**Acid and its concentration used for hydrolysis**			**Temperature**	**Time**
	HCl	**HNO_3**	**CH_3COOH**		
1	0.1M			ambient	24 hours
2	0.1M			85˚C	24 hours
3	1M			ambient	24 hours
4	12M			ambient	48 hours
5		0.1M		ambient	24 hours
6		1M		ambient	24 hours
7			1M	ambient	24 hours

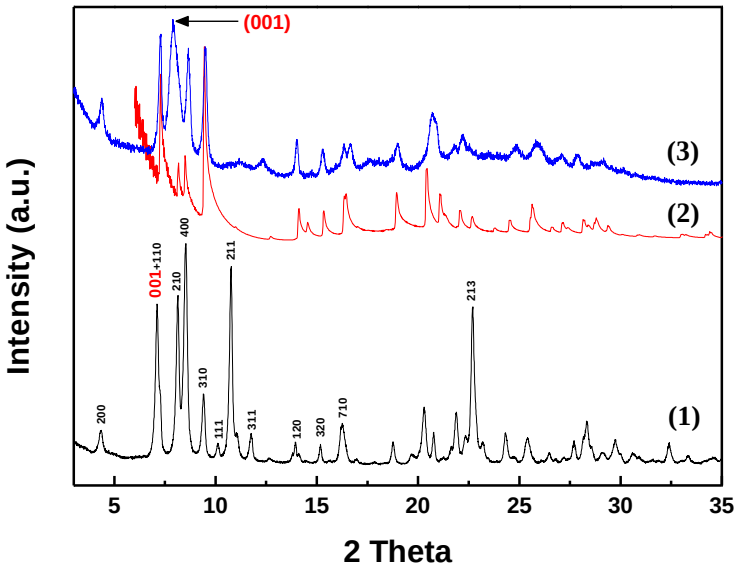

Fig. 25 XRD powder patterns of IWW **(1)** with some reflections indexed with (*hkl*), simulated pattern for a single IWW layer with removed D4R units **(2)** and IWW hydrolysed in 0.1M HCl at room temperature for 43 hours denoted as IPC-5P **(3)**.

Fig. 25 shows the XRD pattern of IWW zeolite with some diffraction lines indexed by Miller indices *hkl* obtained from IZA Web site[7]. The structure of zeolite IWW can be seen as layers separated by D4R units along the *c* axis (**Scheme 5**). In theory, the removal of the D4Rs changes the framework in the *c* axis direction. Consequently, the XRD reflections (*hkl*) with *l* value not equal to zero, for instance (001), (111), (211) or (311), should be changed. The XRD pattern of Ge-rich IWW hydrolysed in 0.1M HCl confirms the presumptions (**Fig. 25**). The most noticeable change is a disappearance of the peaks (111), (211), (311) and from others for instance (213). Unfortunately, the interlayer peak (001), which should be shifted to higher 2θ values (indicating decreasing of the interlayer distance), overlaps with the reflection (110) and hence only the intensity of the peak decreased.

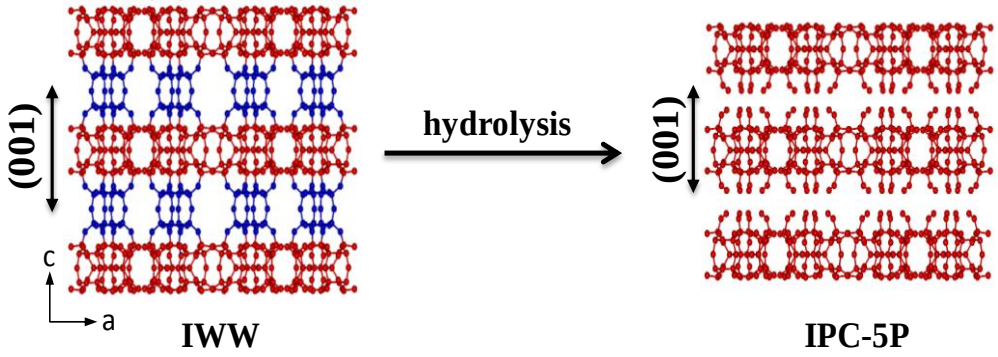

Scheme 5 Schematic view on the 3D-2D transformation of zeolite IWW into layered IPC-5P. The 'layers' in the 3D IWW structure (left) are shown in red and D4R units are shown in blue.

Fig. 25 shows the comparison of the hydrolysed IWW with the simulated XRD pattern for a single IWW layer with removed D4R units. The simulation cannot predict the new position of interlayer (001) because of unknown interactions between the layers. Nevertheless the positions of the peaks correspond pretty well with the experimental data. As the new interlayer reflection (001) attributed to layer stacking was identified the peak appearing in the range from 7.65-8.78˚ (2θ). Its position depends on the hydrolysis conditions (**Table 7, Fig. 26**). Unlike from UTL, the higher temperature led to faster destruction of IWW crystals (**Fig. 26 (2)**) hence, the ambient temperature was found the most suitable for selective disassembly of IWW. The shift of interlayer (001) peak from its original position at 6.97˚ (2θ) (in parent IWW) indicates a contraction of the interlayer space about 0.1-0.3 nm. The removing of most Ge atoms was confirmed by EDX analysis when Si/Ge molar ratio increased from 3.1 up to 45.9. The material prepared by hydrolysis of Ge-rich IWW was denoted IPC-5P, a novel lamellar material with IWW structure of the layers.

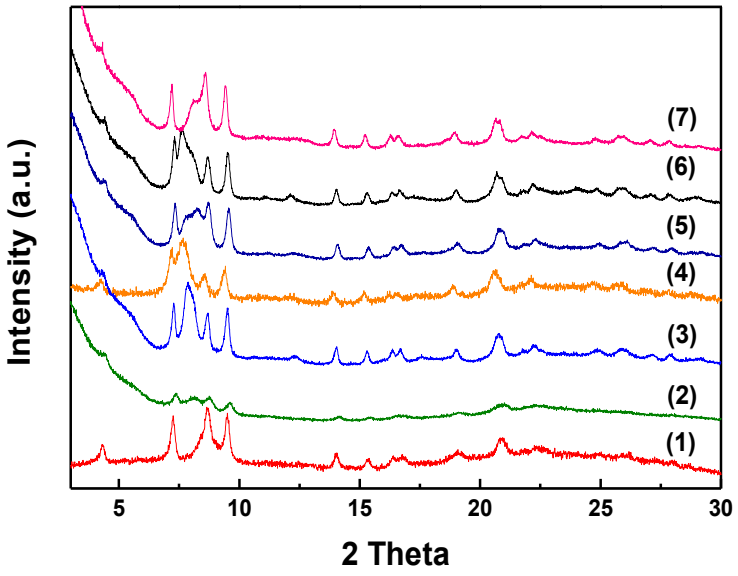

Fig. 26 XRD patterns of hydrolysed Ge-rich IWW (Si/Ge 3.1-3.6) under various conditions described in **Table 7**.

Conversely, the hydrolysis of Ge-poor IWW (Si/Ge 6.4) did not lead to such distinctive structural changes. The comparison of Ge-rich IWW and Ge-poor IWW hydrolysed under the same conditions (0.1M and 12M HCl) indicates that the strength of the acid solution does not really affect the structure of Ge-poor IWW (**Fig. 27**). Nonetheless, the both XRD patterns are slightly distinct from the parent IWW showing that some chemical changes occurred. No shift of interlayer reflections was observed, however, some peaks changed their intensities. The peaks like (111) and (211) remain visible. Similar observations were recently published by Tuel et al., although, they applied the acid treatment on the as-synthesized IWW with SDA molecules present in the pores[75].

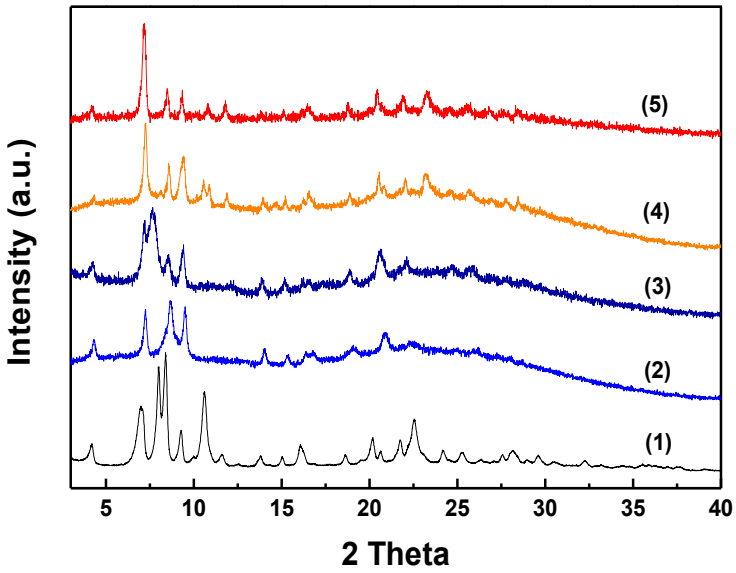

Fig. 27 XRD pattern of calcined IWW **(1)** in comparison with Ge-rich IWW hydrolysed in 0.1M HCl **(2)** and 12M HCl **(3)**, and Ge-poor IWW hydrolysed in 0.1M HCl **(4)** and 12M HCl **(5)**.

The Si/Ge ratio increased from 6.4 in parent IWW up to 50.9 and 121.5 for hydrolysis in 0.1M and 12M HCl, respectively. In spite of the germanium extraction from D4Rs it suggests that the material was not fully hydrolysed into layers and the structure still keeps together forming a defective IWW-like material (**Scheme 6**).

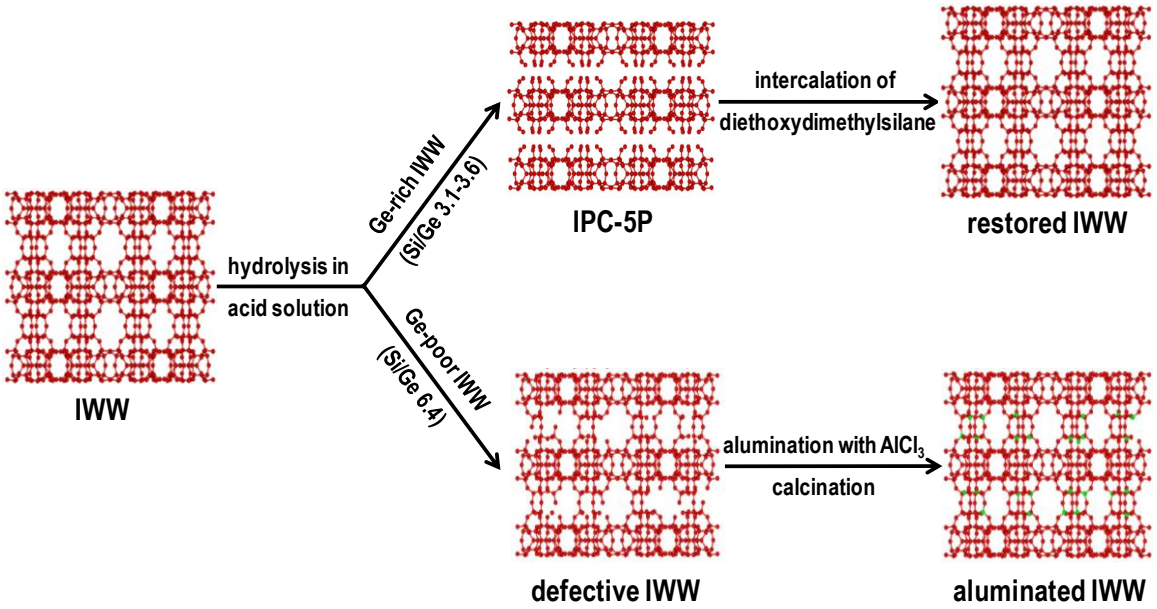

Scheme 6 The schematic view on the hydrolysis of IWW with different germanium content and the post-synthesis treatments leading to the restoring of IWW framework with different chemical composition. Aluminium atoms are in green colour.

Similarly to UTL and its layered IPC-1P, the layered IPC-5P was treated with the solution of hexadecyltrimethylammonium in attempt to increase the interlayer space. In contrast with swollen IPC-1SW, in most of swelling experiments a partial or total dissolution of the zeolite was observed. It is the effect of high pH environment and presence of long-chain organic surfactant like C_{16}TMA resulting in a creation of mesopore particles of M41S type. To avoid the degradation IPC-5P was treated with the mixture of C_{16}TMA-Cl/OH at lower temperature (ice-cooling bath) only for 7 hours. Still, the partial dissolution was not prevented. Unlike the IPC-1P, IPC-5P still possesses 12-8-ring channels going through the layers (sinusoidal 10-ring channels were removed). The porosity of the layers most probably decreases their stability, especially under the basic conditions.

In the surfactant-treated IPC-5P, designated as IPC-5SW, the interlayer reflection (001) (in IPC-5P at 7.8˚ (2θ)) is shifted to lower 2θ values and overlaps with the peak at 7.2˚ (2θ) (**Fig. 28**). The new reflections appeared in the area 10-35˚ (2θ) (marked with asterisks in **Fig. 28**). A partial dissolution of IPC-5P during the swelling (*vide supra*) led to a rearrangement of the species not just into mesopore particles outside the zeolite crystals but as well to rearrangement of atoms between the zeolitic layers. The XRD pattern of IPC-5SW is very similar to parent IWW. However, when a part of IPC-5SW was calcined, the structure collapsed. Only negligible intensities are observed and a big broader band around 2.2˚ (2θ) revealing the presence of mesopores (**Fig. 28**). Overall, due to a relatively small shift of (001) reflection after swelling (only about 0.12 nm), the surfactant is supposed not to be stacked perpendicular to the layers like in IPC-1SW, but might be horizontally between them or does not enter the interlayer space at all.

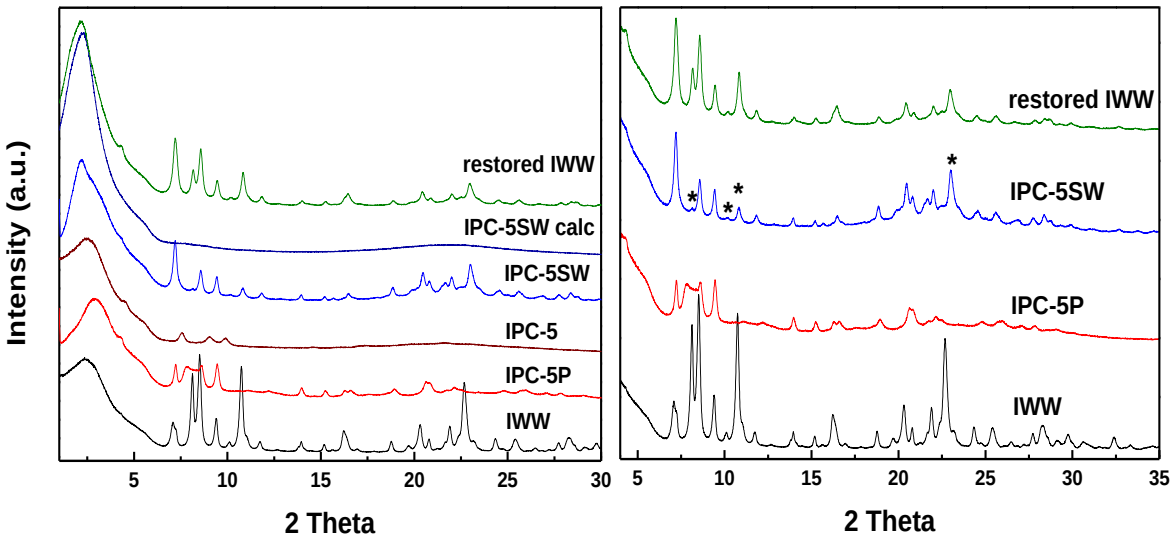

Fig. 28 XRD patterns of IPC-5 family prepared from Ge-rich IWW. On the right side is the closer view on the range 4-35˚ (2θ). Some of the reflections newly appeared after swelling treatment are marked with asterisks.

Assuming the IPC-5SW structure is not stable enough (collapsing after calcination) and there exist some structural defects, IPC-5SW was treated with diethoxydimethylsilane (DEDMS). The same procedure was used for IPC-1P where it led to a formation of new linkages between the layers (new S4R) and the structure of IPC-2 zeolite. In the case of silylated IPC-5SW, after calcination the material gives a very similar XRD pattern as the parent IWW with reflections slightly shifted to higher (2θ) values (**Fig. 28**). The material was designated as restored IWW. Removing of most Ge atoms from the framework and replacing it by Si atoms led to the small decrease in the unit cell size. The EDX analysis confirmed the highly silica material when Si/Ge ratio increased from 3.1 in parent IWW up to 73.4 in the restored IWW.

The layered IPC-1P prepared via hydrolysis from zeolite UTL was possible to directly intercalate with DEDMS or octylamine and after subsequent calcination two new zeolites were formed, IPC-2 and IPC-4, respectively. In the case of layered IPC-5P, no such effect was observed. The direct intercalation of DEDMS and octylamine (without previous swelling step) led to materials with low intensive XRD patterns very similar to hydrolysed calcined Ge-rich IWW denoted as IPC-5 (**Fig. 29**).

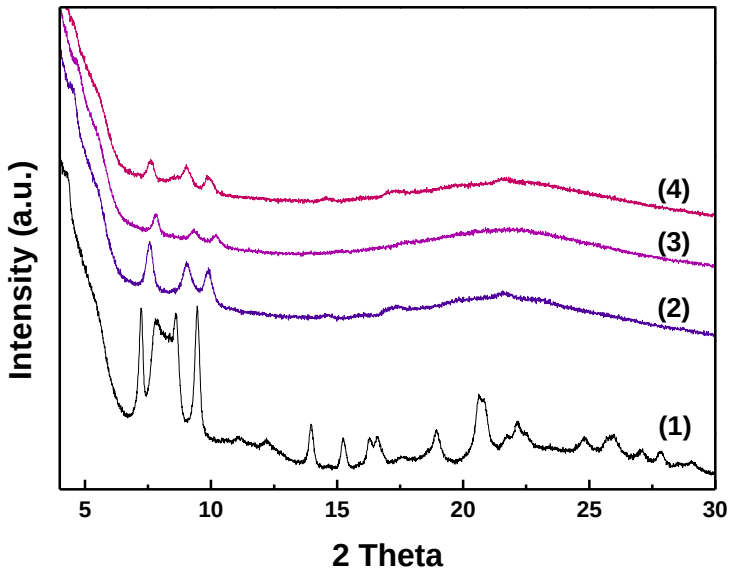

Fig. 29 XRD pattern of hydrolysed IPC-5P **(1)**, calcined hydrolysed IPC-5 **(2)** in comparison with IPC-5P directly intercalated with octylamine (calcined) **(3)** and with DEDMS (calcined) **(4)**.

The structural and textural changes caused by 3D-2D-3D transformation of IWW were investigated by argon adsorption measurement (**Table 8**, **Fig. 30**). The parent IWW (**Fig. 30A**) is a typical microporous zeolite with BET surface area of 416 m^2/g and micropore volume of 0.169 cm^3/g. Its isotherm shows a steep hysteresis loop in the range of relative pressures p/p_0 = 0.9-1.0 explained by a filling of an interparticle space among zeolite crystals, which are of very small sizes < 0.5 μm (*vide infra*). The pore size distribution

Table 8 The chemical composition of individual materials and the textural data from argon sorption measured at (-186 °C).

Material	Si/Ge (EDX)	Argon sorption data		
		BET (m^2/g)	V_{tot} (cm^3/g)	V_{mic} (cm^3/g)
parent IWW	3.1	416	0.169	0.484
IPC-5 calc	45.9	124	0.030	0.213
IPC-5SW calc	-	279	0.015	0.278
restored IWW	73.4	510	0.146	0.450

showed in **Fig. 30B,C** is centred at 0.65 nm corresponding to the presence of 12-10-8-ring channel system of IWW. After hydrolysis in acid solution, the decrease in the adsorbed amount of argon (**Fig. 30A**) indicates that the surface area as well as micropore and total pore volume are greatly reduced to 124 m^2/g, 0.030 and 0.213 cm^3/g, respectively. It correlates with the presumption of hydrolysed IWW where D4R units were destroyed and removed. Before sorption measurement, the hydrolysed sample was calcined at 550 ˚C. The removing of adsorbed water causes the contraction of the interlayer space, which was also recognized in X-ray powder diffraction (see IPC-5 **Fig. 28**). The pore size distribution in **Fig. 30B,C** centred at 0.63 nm has significantly smaller differential pore volume in comparison to parent IWW as the sinusoidal 10-ring channels were removed. However, the layers themselves still possess 12-8-ring channels going through the layers and the material has still a micropore volume 0.030 cm^3/g. Ideally after swelling treatment and calcination, the material should provide similar textural properties as hydrolysed calcined material. Unfortunately, as it was recognised from XRD pattern, during the treatment in a highly basic solution, a part of the zeolite was dissolved and recrystallized into mesopore particles. In the IPC-5SW-calcined isotherm (**Fig. 30A**) the continuous uptake of argon in the range of p/p_0 0.02-0.40 corresponds to the filling of small mesopores. The BET surface area is higher in comparison to hydrolysed IPC-5, 279 cm^3/g, and the total pore volume increased up to 0.278 cm^3/g. Still, some microporosity retained, V_{mic} = 0.015 cm^3/g. The creation of mesopore particles is nicely evidenced by pore size distribution with a large band centred at 3 nm (**Fig. 30B**). After intercalation of diethoxydimethlsilane and restoring of IWW structure the filling of micropores takes place in the low relative pressure region and then it continues in the filling of mesopores. The BET surface area increased up to 510 m^2/g and as the 10-ring channel system was rebuilt, the micropore volume increased up to 0.146 cm^3/g being close to its original value in parent IWW (0.169 cm^3/g). The pore size distribution revealed an intensive band centred at 0.63 nm near its original position in the parent IWW material (0.65 nm) and a broader band centred at 3.2 nm coming from mesopore particles.

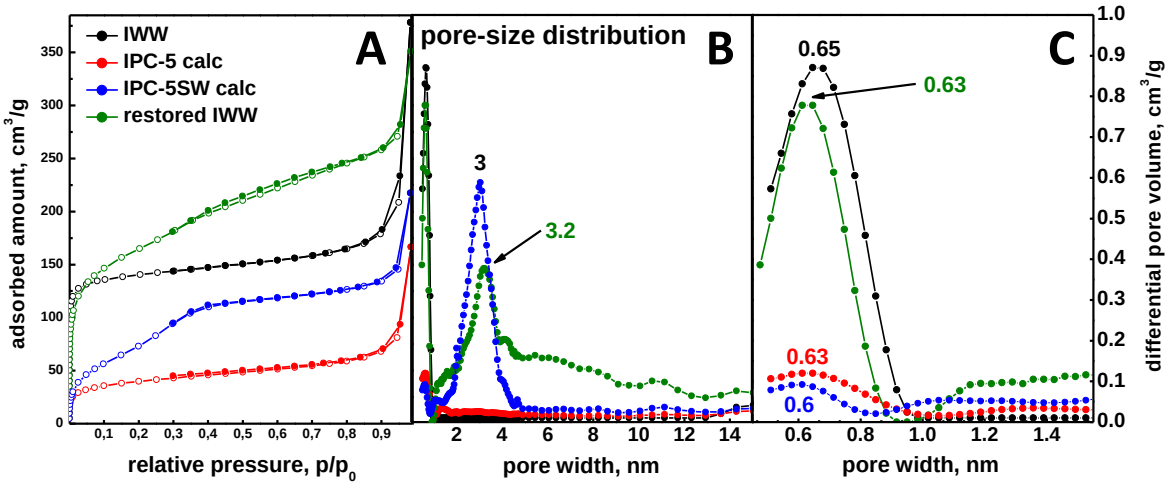

Fig. 30 Adsorption isotherms of argon measured at -186˚C **(A)**. The solid points denote desorption. The pore size distribution in the range between 0-15 nm **(B)**, the closer view on the range 0.5-1.5 nm **(C)**.

In contrast to zeolite UTL the crystals of parent IWW are more ten fifty times smaller. IWW crystallizes as rods of the size below 0.5 μm (**Fig. 31**, **Fig. 32a**). The microstructure of hydrolysed IPC-5P was studied by transmission electron microscopy (HRTEM). The images confirm the layered character of IPC-5P and stacking of the layers along *c* axis (**Fig. 32b,c**).

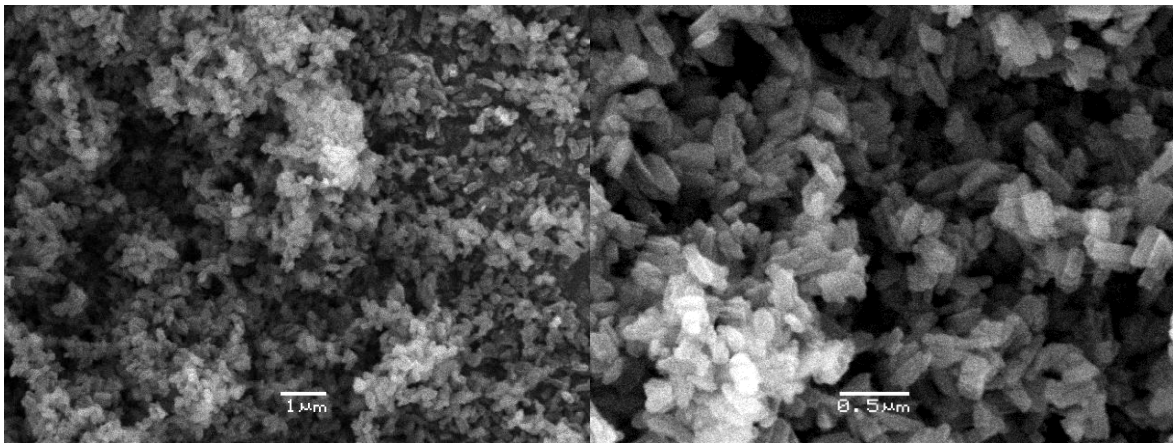

Fig. 31 SEM images from parent IWW zeolite under magnification 30 000 (left) and 60 000 (right).

To confirm the structural changes in IWW during hydrolysis and restoring of IWW structure ^{29}Si solid state MAS NMR spectra were collected (**Fig. 33**). The parent IWW (Si/Ge molar ratio 3.1) exhibits two separated resonances, at -110pm and -113pm. The signal at -113 pm is assigned to pure Si Q^4 groups while the signal at -110 ppm corresponds to Si Q^4 surrounded by at least 1 Ge atom[75,76]. After hydrolysis the resonance at -110 ppm disappeared as Ge atoms in D4R units are removed (Si/Ge molar ratio

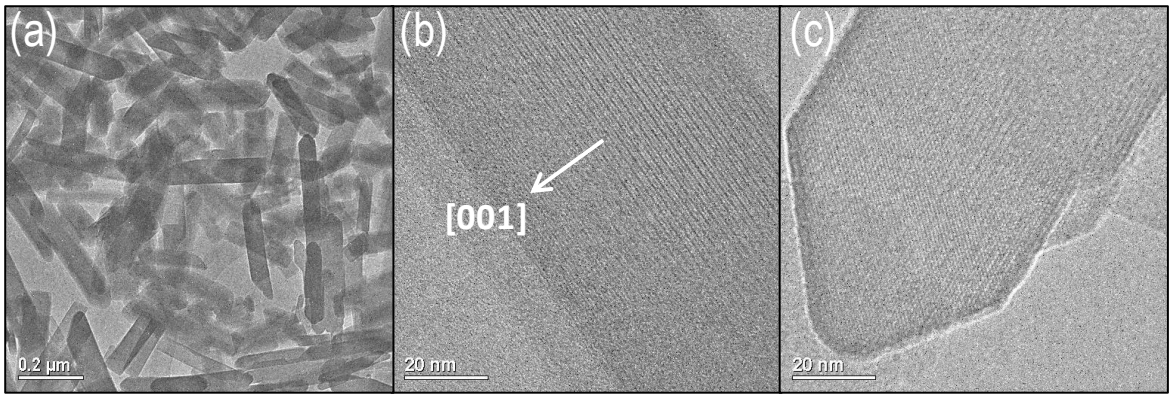

Fig. 32 TEM images of parent IWW zeolite (a) and the hydrolysed layered IPC-5P (b), (c).

increased from 3.1 to 45.9). In addition, a new resonance is observed around -102 ppm, which is commonly assigned to Q^3 signal coming from silanol defects[75,77]. A small signal around -92 ppm attributed to Q^2 was found. After intercalation of DEDMS and restoring of IWW structure Q^2 signal disappeared and Q^3 signal is only of a very small intensity (shoulder) evidencing that most of silanol groups condensed back to Q^4.

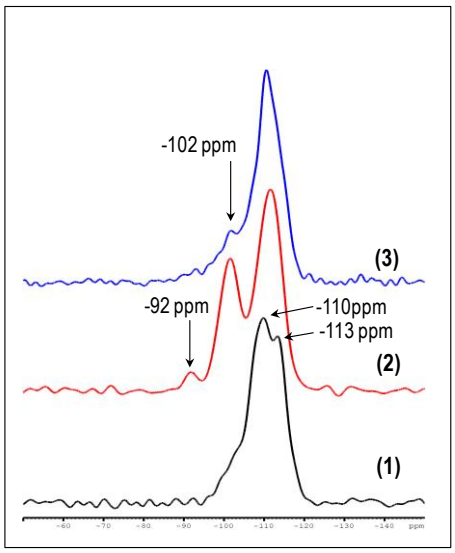

Fig. 33 ^{29}Si MAS NMR data for parent Ge-rich IWW **(1)**, after hydrolysis IPC-5P **(2)** and final restored IWW structure **(3)**.

The existence of structural defects in hydrolysed Ge-poor IWW gives an opportunity to incorporate the catalytic active heteroelement and restore IWW with distinct chemical composition. The incorporation of aluminium was performed on both Ge-rich and Ge-poor hydrolysed IWW using $AlCl_3$ as the source of aluminium (**Fig. 34**). The aluminated Ge-rich material possesses peaks of low intensity (Si/Ge ratio increased from 3.6 up to 101.5). In contrast, the aluminated Ge-poor IWW shows the same architecture as the parent IWW. The differences in alumination of Ge-rich and Ge-poor hydrolysed IWW can be explained as follows. When the D4R units are removed, like in the case of Ge-rich IWW,

the interlayer connections cannot be rebuild using only aluminium atoms as it would break Löwenstein´s rule (Al-O-Al linkages cannot occur). However, in the Ge-poor IWW the hydrolysis led only to defects in the D4Rs. In that case aluminium can be incorporated into the defects and restore IWW structure with new chemical composition (Si/Ge 114.8 and Si/Al 26.9, **Scheme 6**). The presence of aluminium was confirmed by ^{27}Al MAS NMR (**Fig. 35**). A major resonance at 57 ppm indicates the existence of tetrahedrally coordinate aluminium in the framework while the minor signal at 0 ppm comes from a small amount of octahedrally-coordinated Al, extra-framework aluminium species[55,78].

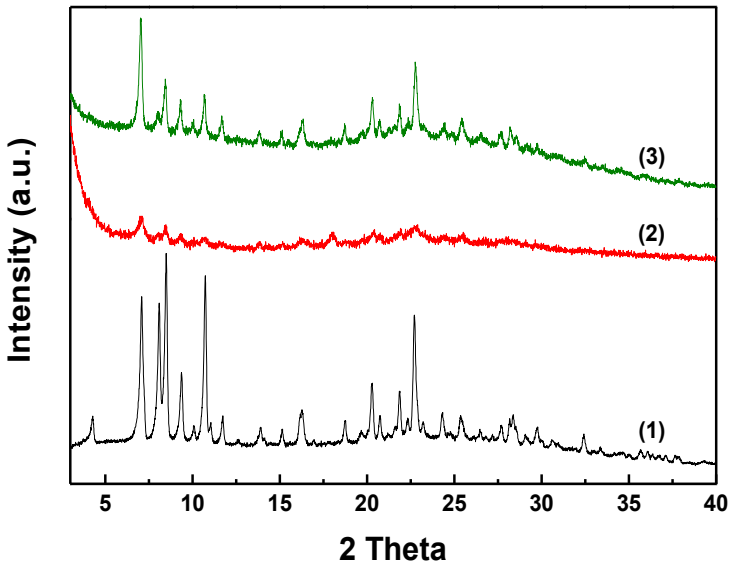

Fig. 34 XRD patterns of IWW zeolite **(1)** in comparison with aluminated hydrolysed Ge-rich IWW **(2)** and aluminated hydrolysed Ge-poor IWW **(3)**.

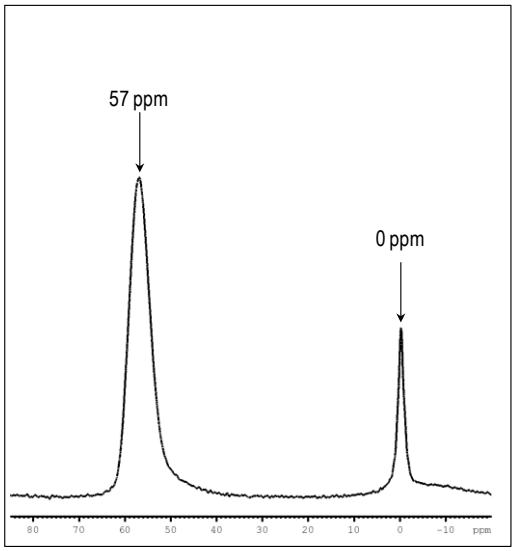

Fig. 35 ^{27}Al MAS NMR data for aluminated sample prepared from hydrolysed Ge-poor IWW.

In conclusion, the application of the ADoR strategy was exemplified on another zeolitic structure, IWW. Unlike UTL where the hydrolysis was effective in the range of Si/Ge ratio 4.0-6.5, in the zeolite IWW the location and the amount of Ge in the D4Rs significantly influence the structure stability in acid environment. Ge-rich IWW was fully disassembled into two-dimensional material, IPC-5P, while hydrolysis of Ge-poor IWW led to a defective IWW structure preserving some interlayer connections. The layered IPC-5P was converted back to the three-dimensional structure of IWW by incorporation of silylating agent. In contrast to the zeolite UTL and its IPC-1P, the layered structure of IPC-5P strongly tends to a formation of its original IWW framework. Based on the results the general application of the ADoR concept was confirmed.

The structural defects in Ge-poor IWW, caused by acid hydrolysis, were filled via incorporation of Al. Considering the extraction of Ge atoms from D4R units aluminium atoms were most probably incorporated into defined crystallographic positions – in D4Rs. Thus, the accessibility to acid sites was most probably increased in comparison to directly synthesized Al-IWW where aluminium atoms are located mainly in layers themselves.

5 Conclusions

The PhD thesis deals with the synthesis of novel zeolite materials, investigation of their properties (structural, textural, acid ones) and their possible use in catalytic application. The work was focused on the two-dimensional zeolites having typically one dimension significantly limited to 1 or less unit cell size.

Zeolite UTL was prepared as a pure germanosilicate with Si/Ge ratio 4.0-6.5. It was found that UTL undergoes unique structural changes in the neutral or slightly acid environment leading to transformation from three-dimensional framework into two-dimensional layered material. Zeolite UTL is the first example of the 3D-2D zeolite transformation, so called top-down synthesis, with the preservation of the original character of the layers. The UTL degradation proceeds due to the presence of double-four-units (D4Rs), which can be seen as supporting units/pillars between the rigid layers. The preferential location of Ge in D4Rs make the units an ideal target for their selective removal as the Ge-O-Ge bonds are less hydrolytically stable then Si-O-Si. The degradation of D4Rs during the hydrolysis in water or 0.1M HCl at temperatures close to boiling point led to the formation of layered material, denoted IPC-1P, comprises mostly of silica and oxygen atoms and without any channel system.

The interlayer space in IPC-1P was modified by introduction of long-organic chain surfactant (hexadecyltrimethylammonium) during the swelling treatment. In the swollen IPC-1SW the interlayer space was enlarged from 0.1-0.2 nm (in IPC-1P) up to 2.5 nm. To keep the interlayer space permanently expanded and to prevent the contraction after calcination, the silica amorphous pillars were subsequently introduced. The pillared material, IPC-1PI, exhibited distinctively enhanced BET surface area (up to 1100 m^2/g) and total pore volume (up to 0.8 cm^3/g).

During all post-synthesis treatments of UTL, the integrity and the original character of the UTL-like layers remained as it was confirmed by electron diffraction and high resolution transmission electron microscopy.

The individual layers in IPC-1P were condensed back and formed new structures. Depending on the chosen linkage, two novel zeolites were prepared - IPC-2 and IPC-4. The original D4R units in UTL were replaced by new single-four-ring (S4R) units in IPC-2 or by single Si-O-Si bridges in IPC-4. Three zeolites are structurally related since they have the same UTL-like layers and differ only in the layer linkers. The size of their channel systems decreases with the size of the linkage in order: UTL (14-12-ring) > IPC-2 (12-10-ring) > IPC-4 (10-8-ring). The trend was confirmed by argon sorption measuring when both BET surface areas and micropore volumes decreased with decreasing size of the channel system.

IPC-2 and IPC-4 were verified by IZA Structure Commission as novel zeolites with three letter codes OKO (for COK-14, which is isostructure to IPC-2) and PCR (Prague

Chemistry fouR), respectively. Zeolite PCR is the first zeolite prepared in the Czech Republic.

The new approach for the design and synthesis of zeolites was denoted the ADoR strategy. The abbreviation means that first it is necessary to synthesize the parent zeolite - **A**ssembly, then hydrolyse it into layered material – **D**isassembly, followed by **o**rganisation of the layers and finally calcination into new material – **R**eassembly. The novel synthetic strategy enables to prepare zeolites with predetermined pore architecture as it depends on the chosen linker between the layers. The different pore sizes and structures control the accessibility to the internal surface of zeolites, and thus it significantly influences their catalytic performance. Moreover, the hydrothermally unstable zeolite UTL was used to prepare two more stable zeolites when most of Ge atoms were removed and partially replaced by Si atoms.

The mechanism of the ADoR was studied in detail under various hydrolysis conditions: neutral pH of water, acid conditions of 0.1M-12M hydrochloric acid. It was found that the first minutes of hydrolysis, disassembly of UTL, did not depend on the environment (specifically pH) and led to removal of most Ge atoms. Afterwards two processes of de-intercalation and rearrangement compete and the crucial factor is the H^+ concentration. The neutral or slightly acid conditions (water or 0.1M HCl) favour the removal of species between the layers – de-intercalation. Conversely, the highly concentrated HCl favours the rearrangement of atoms between the layers. The end products are zeolites IPC-4 (in the case of the de-intercalation) and IPC-2 (in the case of the rearrangement). Using a specific HCl concentration (1.5M) it can be reached the equilibrium between the rate of de-intercalation and rearrangement when half of the layers undergoes the de-intercalation and the rest undergoes the rearrangement. Reassembly of the material led to a new material designated IPC-6. IPC-6 can be seen as a structural combination of IPC-2 and IPC-4 zeolites with two independent pore systems of 12-10-ring and 10-8-ring size.

The novel materials, IPC-1PI, IPC-2 and IPC-4, were also prepared in the catalytic active forms containing aluminium. They were tested in the alkylation of toluene with isopropyl alcohol and the results were compared with Al-UTL and commercial zeolites Al-BEA and Al-MFI. Using pillared Al-IPC-1PI was achieved higher toluene conversions in comparison to Al-IPC-2, which was in time faster deactivated by coking. The selectivities to cymenes over Al-IPC-1PI and Al-IPC-2 were similar. The *para*-selectivity over Al-IPC-2 reached 67%, which is similar to Al-MFI 72%, while over Al-IPC-1PI it was only 45% (at the 5% conversion of toluene). The pillared Al-IPC-1PI was found to act similar to solid acids, like e.g. $AlCl_3$, because the layers do not possess any micropores and thus the active sites can only be located on the layer surface. Al-IPC-4 did not provide practically any activity. It is explained by the small 10-8-ring channel system where the aromatic molecules can hardly diffuse. The pillared Al-IPC-1PI was additionally tested in the reaction of styrene with phenol/*tert*-butylphenol and the results were compared to

commercial Al-BEA. In the reaction of styrene with bulkier molecule of *tert*-butylphenol the higher conversion of styrene was achieved over pillared Al-IPC-1PI. It turned out that the enhanced accessibility to active sites for bulky molecules is more important than the concentration or type of acid sites.

The ADoR concept was successfully applied on other zeolite, germanosilicate IWW. Unlike UTL where the hydrolysis was effective in the range of Si/Ge ratio 4.0-6.5, in the zeolite IWW the location and amount of Ge in the D4Rs significantly influenced the structure stability in acid environment. Ge-rich IWW (Si/Ge molar ratio 3.1-3.6) was fully disassembled into two-dimensional material IPC-5P. In contrast to zeolite UTL, the influence of variously strong acid solutions was not observed. The layered IPC-5P was converted back to the three-dimensional structure of IWW by incorporation of silylating agent. Apart from the zeolite UTL and its IPC-1P, the layered structure of IPC-5P strongly tends to a formation of its original IWW framework. The 3D-2D-3D transformation of zeolite framework is a very unique case, which until now has not been described. Thus, the general application of the ADoR concept was confirmed.

The hydrolysis of Ge-poor IWW (Si/Ge 6.4) led to a defective IWW structure preserving some interlayer connections. The structural defects in Ge-poor IWW, caused by extraction of Ge atoms during the acid treatment, were filled via incorporation of aluminium atoms, which are most probably located in the D4R units where are easily accessible.

6 References

1 A. Pulido, P. Nachtigall, A. Zukal, I. Dominguez, J. Čejka, *J. Phys. Chem. B*, 113 (**2009**) 2929

2 M. Bejblová, D. Procházková, J. Čejka, *ChemSusChem*, 2 (**2009**) 486

3 N. Žilková, M. Bejblová, B. Gil, S.I. Zones, A. Burton, C.Y. Chen, Z. Musilová-Pavlačková, G. Košová, J. Čejka, *J. Catal.*, 226 (**2009**) 79

4 J. Čejka, A. Corma, S. Zones (Eds.), *Zeolites and Catalysis: Synthesis, Reactions and Apllications*, Vol. 2, Wiley-VCH: Weinheim, **2010**

5 M.E. Davis, *Nature*, 417 (**2002**) 813

6 W. Han, S.M. Kwan, K.L. Yeung, *Top. Catal.*, 53 (**2010**) 1394

7 IZA Structure Commission Web site, http://www.iza-structure.org/default.htm

8 S.M. Csicsery, *Zeolites*, 4 (**1984**) 202

9 E.M. Flanigen in *Introduction to Zeolite Science and Practice*, 2nd Ed.; H. van Bekkum, E.M. Flanigen, P.A. Jacobs, J.C. Jensen, Eds.; *Stud. Surf. Sci. Catal.*, Elsevier: Amsterdam, **2001**, Vol. 137, p. 11

10 R.M. Barrer, *J. Chem. Soc.*, (**1948**) 2158

11 T.B. Reed, D.W. Breck, *J. Am. Chem. Soc.*, 78 (**1956**) 5972

12 R.M. Milton, US Patent 2,882,244 (**1959**)

13 D.W. Breck, US Patent 3,130,007 (**1974**)

14 R.M. Barrer, P.J. Denny, *J. Chem. Soc.*, (**1961**) 971

15 B.M. Lok, T.R. Cannan, C.A. Messina, *Zeolites*, 3 (**1983**), 282

16 J. Čejka in *Encyclopedia of Supramolecular Chemistry*; J.L. Atwood, J.W. Steed, Eds.; Taylor & Francis Group: Suine, **2004**, p. 1623

17 N.Y. Chen, T.F. Degnan, C.M. Smith, *Molecular transport and reaction in zeolites*, John Wiley&Sons: New York, **1994**

18 R.M. Barrer, *Hydrothermal Chemistry of Zeolites*, Academic Press, New York, **1982**

19 J. Čejka, H. van Bekkum, A. Corma, F. Schüth (Eds.), *Introduction to zeolite science and practise*, 3rd Ed.; *Stud. Surf. Sci. Catal.*, Elsevier: Amsterdam, **2007**, Vol. 168

20 J.C. Groen, W. Zhu, S. Brouwer, S.J. Huynink, F. Kapteijn, J.A. Moulijn, J. Pérez-Ramírez, *J. Am. Chem. Soc.*, 129 (**2007**) 355

21 O.C. Gobin, S.J. Reitmeier, A. Jentys, J.A. Lercher, *J. Phys. Chem. C*, 113 (**2009**) 20435

22 D. Theodorou, J. Wei, *J.Catal.*, 83 (**1983**) 205

23 W.J. Roth, J. Čejka, *Catal. Sci. Technol.*, 1 (**2011**) 43

24 M.E. Leonowicz, J.A. Lawton, S.L. Lawton, M.K. Rubin, *Science*, 264 (**1994**) 1910

25 S.L. Lawton, A.S. Fung, G.J. Kennedy, L.B. Alemany, C.D. Chang, G.H. Hatzikos, D.N. Lissy, M.K. Rubin, H.-K.C. Timken, *J. Phys. Chem.*, 100 (**1996**) 3788

26 S. Zanardi, A. Alberti, G. Cruciani, A. Corma, V. Fornés, M. Brunelli, *Angew. Chem., Int. Ed.*, 43 (**2004**) 4933
27 W.L. Shreyeck, P. Caullet, J.C. Mougenel, J.L. Guth, B. Marler, *J. Chem. Soc.*, (**1995**) 2187
28 U. Oberhagenmann, P. Bayat, B. Marler, H. Gies, J. Rius, *Angew. Chem., Int. Ed.*, 35 (**1996**) 2869
29 B. Marler, M.A. Camblor, H. Gies, *Microporous Mesoporous Mater*., 90 (**2006**) 87
30 B. Marler, N. Ströter, H. Gies, *Microporous Mesoporous Mater*., 83 (**2005**) 201
31 Y. Wang, B. Marler, H. Gies, U. Müller, *Chem. Mater.*, 17 (**2005**) 43
32 P.S. Wheatley, R.E. Morris, *J. Mater. Chem.*, 16 (**2006**) 1035
33 T. Ikeda, Y. Akiyama, Y. Oumi, A. Kawai, F. Mizukami, *Angew. Chem., Int. Ed.*, 43 (**2004**) 4892
34 D.L. Dorset, G.J. Kennedy, *J. Phys. Chem. B*, 108 (**2004)** 15216
35 M. Choi, K. Na, J. Kim, Y. Sakamoto, O. Terasaki, R. Ryoo, *Nature*, 461 (**2009**) 246
36 J. Jung, C. Jo, K. Cho, R. Ryoo, *J. Chem. Mater.*, 22 (**2012**) 4637
37 W.J. Roth, C.T. Kresge, J.C. Vartuli, M.E. Leonowicz, A.S. Fung, S.B. McCullen in *Catalysis by microporous materials;* H.K. Beyer, H.G. Karge, I. Kiricsi, J.B. Nagy, Eds.; *Stud. Surf. Sci. Catal*, Elsevire: Amsterdam, **1995**, Vol. 94, p. 301
38 W.J. Roth, D. L. Dorset, *Microporous Mesoporous Mater*., 142 (**2011**) 32
39 W.J. Roth in *Introduction to Zeolite Science and Practice*, 3rd Ed.; J. Čejka, H. van Bekkum, A. Corma, F. Schüth, Eds.; *Stud. Surf. Sci. Catal.*, Elsevier: Amsterdam **2007**, Vol. 168, p. 221
40 A. Corma, V. Fornes, S.B. Pergher, T.L.M. Maesen, J.G. Buglass, *Nature*, 393 (**1998**) 353
41 A.S. Fung, S.L. Lawton, W.J. Roth, US Patent 5,362,697 (**1994**)
42 P. Wu, J. Ruan, L. Wang, L. Wu, Y. Wang, Y. Liu, W. Fan, M. He, O. Terasaki, T. Tatsumi, *J. Am. Chem. Soc.*, 130 (**2008**) 8178
43 A. Corma, M.J. Díaz-Cabanas, F. Rey, S. Nicolopoulus, K. Boulahya, *Chem. Commun.*, 12 (**2004**) 1356
44 J.L. Paillaud, B. Harbuzaru, J. Patarin, N. Bats, *Science*, 304 (**2004**) 990
45 C. Baerlocher, W.M. Maier, D.H. Olson, *Atlas of zeolite framework types*, 6th Ed.; Elsevier: Amsterdam, **2007**
46 T. Blasco, A. Corma, M.J. Diaz Cabanas, F. Rey, J.A. Vidal Moya, C.M. Zicovich Wilson, *J. Phys. Chem. B*, 106 (**2002**) 2634
47 . A. Corma, M. Diaz-Cabanas, J. Martinez-Triguero, F. Rey, J. Rius, *Nature*, 418 (**2002**) 514
48 A. Pulido, G. Sastre, A. Corma, *ChemPhysChem.*, 7 (**2006**) 1092
49 D.S. Wragg, R.E. Morris, A.W. Burton, *Chem. Mater.*, 20 (**2008**) 1561
50 O.V. Shvets, N. Kasian, A. Zukal, J. Pinkas, J. Čejka, *Chem. Mater*., 22 (**2010**) 3482

51 M.V. Shamzhy, O.V. Shvets, M.V. Opanasenko, P.S. Yaremov, L.G. Sarkisyan, P. Chlubná, A. Zukal, J. Čejka, *J. Mater. Chem.*, 22 (**2012)** 15793
52 H. Xu, J. Jiang, B. Yang, L. Zhang, M. He, P. Wu, *Angew. Chem., Int. Ed.*, 53 (**2014**) 1355.
53 M.V. Shamzhy, O.V. Shvets, M.V. Opanasenko, L. Kurfiřtová, D. Kubička, J. Čejka, *Chem. Cat. Chem.*, 5 (**2013**) 1891
54 N. Žilková, M. Shamzhy, O. Shvets, J. Čejka, *Catal. Today*, 204 (**2013**) 22
55 A. Corma, F. Rey, S. Valencia, J.L. Jorda, J. Rius, *Nat. Mater.*, 2 (**2003**) 493
56 O.V. Shvets, A. Zukal, N. Kasian, N. Žilková, J. Čejka, *Chem. Eur. J.*, 14 (**2008**) 10134
57 O.V. Shvets, M.V. Shamzhy, P.S. Yaremov, Z. Musilová, D. Procházková, J. Čejka, *Chem. Mater.*, 23 (**2011**) 2573
58 S. Brunauer, P.H. Emmet, E. Teller, *J. Am. Chem. Soc.*, 62 (**1938**) 309
59 B.C. Lippens and J.H. de Boer, *J. Catal.*, 4 (**1965**) 319
60 E.P. Barret, L.G. Joyner, P.B. Halenda, *J. Am. Chem. Soc.*, 73 (**1951**) 373
61 B. Wichterlová, Z. Tvarůžková, Z. Sobalík, P. Sarv, *Microporous Mesoporous Mater.*, 24 (**1998**) 223
62 A. Bergamaschi, A. Cervellino, R. Dinapoli, F. Gozzo, B. Henrich, I. Johnson, P. Kraft, A. Mozzanica, B. Schmitt, X. Shi, *Nucl. Instrum. Methods Phys. Res., Sect. A*, 604 (**2009)** 136
63 W.J. Roth, J.C. Vartuli, C.T. Kresge in *Nanoporous Materials II;* A. Sayari, M. Jaroniec, Eds.; *Stud. Surf. Sci. Catal.*, Elsevire: Amsterdam, **2000**, Vol. 129, p. 501
64 K.S.W. Sing, D.H. Everett, F.A.W. Haul, L. Mouscou, R.A. Pierotti, J. Rouquerol, T. Siemieniewska, *Pure Appl. Chem.*, 57 (**1985**) 603
65 M. Kruk, M. Jaroniec, A. Sayari, *J. Phys. Chem. B*, 101 (**1997**) 583
66 J. Hermann, M. Trachta, P. Nachtigall, O. Bludský, *Catal. Today*, (**2013**) in press, doi: 10.1016/j.cattod.2013.09.016
67 E. Verheyen, L. Joos, K. Van Havenbergh, E. Breynaert, N. Kasian, E. Gobechiya, K. Houthoofd, C. Martineau, M. Hinterstein, F. Taulelle, V. Van Speybroeck, M. Waroquier, S. Bals, G. Van Tendeloo, C.E.A. Kirschhock and J.A. Martens, *Nat. Mater.*, 11 (**2012**) 1059
68 K. Ito, *Hydrocarb. Proc.*, 52 (**1973**) 89
69 (a) W.J. Welstead Jr., *Kirk-Othmer Encyclopedia Chem. Technol.*, 9 (**1978**) 544
(b) J.M. Derfer, M.M. Derfer, *Kirk-Othmer Encyclopedia Chem. Technol.*, 22 (**1978**) 709
70 D. Fraenkel, M. Levy, *J. Catal.*, 118 (**1989**) 10
71 B. Wichterlová, J. Čejka, N. Žilková, *Microporous Mater.*, 6 (**1996**) 405

72 G.A. Olah, R. Krishnamurti, G.K.S. Prakash, *Friedel-Crafts Alkylations in Comprehensive*; *Organic Synthesis;* B.M. Trost, I. Fleming, Eds.; Pergamon Press: Oxford, **1991**, Vol. 3, p. 293
73 A. Hamze, D. Veau, O. Provot, J.D. Brion, M. Alami, *J. Org.Chem.*, 74 (**2009**) 1337
74 I. Jovel, K. Mertins, J. Kischel, A. Zapf, M. Beller, *Angew. Chem., Int. Ed.*, 44 (**2005**) 3913
75 L. Burel, N. Kasian, A. Tuel, *Angew. Chem., Int. Ed.*, 53 (**2014**) 1360
76 H. Kosslick, V.A. Tuan, R. Fricke, C. Peuker, W. Pilz, W. Storek, *J. Phys. Chem.*, 97 (**1993**) 5678
77 T. Blasco, A. Corma, M.J. Díaz-Cabañas, F. Rey, J.A. Vidal-Moya, C.M. Zicovich-Wilson, *J. Phys. Chem. B*, 106 (**2002**) 2634
78 F. Gao, M. Jaber, K. Bozhilov, A. Vicente, C. Fernandez, V. Valtchev, *J. Am. Chem. Soc.*, 131 (**2009**) 16580

7 Enclosures

1) Roth W.J., Shvets O.V., Shamzhy M., Chlubná P., Kubů M., Nachtigall P., Čejka J.;
Postsynthesis Transformation of Three-Dimensional Framework into a Lamellar Zeolite with Modifiable Architecture;
Journal of American Chemical Society, 2011, 133, 6130-6133

2) Shamzhy M.V., Shvets O.V., Opanasenko M.V., Yaremov P.S., Sarkisyan L.G., Chlubná P., Zukal A., Marthala V.R., Hartmann M., Čejka J.;
Synthesis of isomorphously substituted extra-large pore UTL zeolites;
Journal of Materials Chemistry, 2012, 22, 15793-15803

3) Chlubná P., Roth W.J., Greer H.F., Zhou W., Shvets O., Zukal A., Čejka J., Morris R.E.;
3D to 2D routes to ultrathin and expanded zeolitic materials;
Chemistry of Materials, 2013, 25, 542-547

4) Roth W.J., Nachtigall P., Morris R.E., Wheatley P.S., Seymour V.R., Ashbrook A.E., Chlubná P., Grajciar L., Položij M., Zukal A., Shvets O., Čejka, J.;
A family of zeolites with controlled pore size prepared using a top-down method;
Nature Chemistry, 2013, 5, 628-633

5) Mazur M., Chlubná-Eliášová P., Roth W.J., Čejka J.;
Intercalation chemistry of layered zeolite precursor IPC-1P;
Catalysis Today, 2013, in press, doi: 10.1016/j.cattod.2013.10.051